Colley KJ, Lee EU, Adler B, Browne JK, Paulson JC. 1989. Conversion of a Golgi apparatus sialyltransferase to a secretory protein by replacement of the NH2-terminal signal anchor with a signal peptide. *J Biol Chem.* 264:17619–17622.

Colley KJ, Lee EU, Paulson JC. 1992. The signal anchor and stem regions of the beta-galactoside alpha2,6-sialyltransferase may each act to localize the enzyme to the Golgi apparatus. *J Biol Chem.* 267:7784–7793.

Collins BE, Smith BA, Bengtson P, Paulson JC. 2006. Ablation of CD22 in ligand-deficient mice restores B cell receptor signaling. *Nat Immunol.* 7:199–206.

Dall'Olio F, Chiricolo M, Mariani E, Facchini A. 2001. Biosynthesis of the cancer-related sialyl-alpha2,6-lactosaminyl epitope in colon cancer cell lines expressing beta-galactoside alpha2,6-sialyltransferase under a constitutive promoter. *Eur J Biochem.* 268:5876–5884.

Dalziel M, Lemaire S, Ewing J, Kobayashi L, Lau JT. 1999. Hepatic acute phase induction of murine beta-galactoside alpha2,6 sialyltransferase (ST6Gal I) is IL-6 dependent and mediated by elevation of exon H-containing class of transcripts. *Glycobiology.* 9:1003–1008.

Ehehalt R, Keller P, Haass C, Thiele C, Simons K. 2003. Amyloidogenic processing of the Alzheimer beta-amyloid precursor protein depends on lipid rafts. *J Cell Biol.* 160:113–123.

Futakawa S, Kitazume S, Oka R, Ogawa K, Kinoshita A, Miyashita Y, Hashimoto Y. 2009. Development of sandwich enzyme-linked immunosorbent assay systems for plasma β-galactoside α2,6-sialyltransferase, a possible hepatic disease biomarker. *Analytica Chimica Acta.* 631:116–120.

Grewal PK, Boton M, Ramirez K, Collins BE, Saito A, Green RS, Ohtsubo K, Chui D, Marth JD. 2006. ST6Gal-I restrains CD22-dependent antigen receptor endocytosis and Shp-1 recruitment in normal and pathogenic immune signaling. *Mol Cell Biol.* 26:4970–4981.

Heijne WH, Stierum RH, Slijper M, van Bladeren PJ, van Ommen B. 2003. Toxicogenomics of bromobenzene hepatotoxicity: A combined transcriptomics and proteomics approach. *Biochem Pharmacol.* 65:857–875.

Hennet T, Chui D, Paulson JC, Marth JD. 1998. Immune regulation by the ST6Gal sialyltransferase. *Proc Natl Acad Sci USA.* 95:4504–4509.

Hussain I, Powell D, Howlett DR, Tew DG, Meek TD, Chapman C, Gloger IS, Murphy KE, Southan CD, Ryan DM, et al. 1999. Identification of a novel aspartic protease (Asp 2) as beta-secretase. *Mol Cell Neurosci.* 14:419–427.

Kaplan HA, Woloski BM, Hellman M, Jamieson JC. 1983. Studies on the effect of inflammation on rat liver and serum sialyltransferase. Evidence that inflammation causes release of Gal beta 1 leads to 4GlcNAc alpha 2 leads to 6 sialyltransferase from liver. *J Biol Chem.* 258:11505–11509.

Kitagawa H, Paulson JC. 1994. Differential expression of five sialyltransferase genes in human tissues. *J Biol Chem.* 269:17872–17878.

Kitazume S, Nakagawa K, Oka R, Tachida Y, Ogawa K, Luo Y, Citron M, Shitara H, Taya C, Yonekawa H, et al. 2005. In vivo cleavage of alpha2,6-sialyltransferase by Alzheimer beta-secretase. *J Biol Chem.* 280:8589–8595.

Kitazume S, Tachida Y, Oka R, Kotani N, Ogawa K, Suzuki M, Dohmae N, Takio K, Saido TC, Hashimoto Y. 2003. Characterization of alpha2,6-sialyltransferase cleavage by Alzheimer's beta -secretase (BACE1). *J Biol Chem.* 278:14865–14871.

Kitazume S, Tachida Y, Oka R, Shirotani K, Saido TC, Hashimoto Y. 2001. Alzheimer's beta-secretase, beta-site amyloid precursor protein-cleaving enzyme, is responsible for cleavage secretion of a Golgi-resident sialyltransferase. *Proc Natl Acad Sci USA.* 98:13554–13559.

Kitazume-Kawaguchi S, Dohmae N, Takio K, Tsuji S, Colley KJ. 1999. The relationship between ST6Gal I Golgi retention and its cleavage-secretion. *Glycobiology.* 9:1397–1406.

Laemmli UK. 1970. Cleavage of structural proteins during the assembly of the head of bacteriophage T4. *Nature.* 227:680–685.

Lau SS, Monks TJ. 1988. The contribution of bromobenzene to our current understanding of chemically-induced toxicities. *Life Sci.* 42:1259–1269.

Mori M, Yoshida MC, Takechi N, Taniguchi N. 1991. *The LEC Rat, a New Model for Hepatitis and Liver Cancer.* Tokyo: Springer.

Naugler WE, Sakurai T, Kim S, Maeda S, Kim K, Elsharkawy AM, Karin M. 2007. Gender disparity in liver cancer due to sex differences in MyD88-dependent IL-6 production. *Science.* 317:121–124.

Recchi MA, Hebbar M, Hornez L, Harduin-Lepers A, Peyrat JP, Delannoy P. 1998. Multiplex reverse transcription polymerase chain reaction assessment of sialyltransferase expression in human breast cancer. *Cancer Res.* 58:4066–4070.

Seglen PO. 1976. Preparation of isolated rat liver cells. *Methods Cell Biol.* 13:29–83.

Semel AC, Seales EC, Singhal A, Eklund EA, Colley KJ, Bellis SL. 2002. Hyposialylation of integrins stimulates the activity of myeloid fibronectin receptors. *J Biol Chem.* 277:32830–32836.

Simons M, Keller P, De Strooper B, Beyreuther K, Dotti CG, Simons K. 1998. Cholesterol depletion inhibits the generation of beta-amyloid in hippocampal neurons. *Proc Natl Acad Sci USA.* 95:6460–6464.

Sinha S, Anderson JP, Barbour R, Basi GS, Caccavello R, Davis D, Doan M, Dovey HF, Frigon N, Hong J, et al. (1999) Purification and cloning of amyloid precursor protein beta-secretase from human brain. *Nature.* 402:537–540.

Sugimoto I, Futakawa S, Oka R, Ogawa K, Marth JD, Miyoshi E, Taniguchi N, Hashimoto Y, Kitazume S. 2007. ST6Gal I cleavage by BACE1 enhances the sialylation of soluble glycoproteins: A novel regulatory mechanism for alpha2,6-sialylation. *J Biol Chem.* 282:34896–34903.

Suzuki K, Miyazawa N, Nakata T, Seo HG, Sugiyama T, Taniguchi N. 1993. High copper and iron levels and expression of Mn-superoxide dismutase in mutant rats displaying hereditary hepatitis and hepatoma (LEC rats). *Carcinogenesis.* 14:1881–1884.

Varki A. 1999. Sialic acids. In: Varki A, Cummings R, Esko J, Freeze H, Hart G, Marth J, editors. *Essentials of Glycobiology.* Cold Spring Harbor, New York: Cold Spring Harbor Laboratory Press. p. 195–209.

Vassar R, Bennett BD, Babu-Khan S, Kahn S, Mendiaz EA, Denis P, Teplow DB, Ross S, Amarante P, Loeloff R, et al. 1999. Beta-secretase cleavage of Alzheimer's amyloid precursor protein by the transmembrane aspartic protease BACE [see comments]. *Science.* 286:735–741.

Weinstein J, Lee EU, McEntee K, Lai PH, Paulson JC. 1987. Primary structure of beta-galactoside alpha2,6-sialyltransferase. Conversion of membrane-bound enzyme to soluble forms by cleavage of the NH2-terminal signal anchor. *J Biol Chem.* 262:17735–17743.

Wu J, Forbes JR, Chen HS, Cox DW. 1994. The LEC rat has a deletion in the copper transporting ATPase gene homologous to the Wilson disease gene. *Nat Genet.* 7:541–545.

Wuensch SA, Huang RY, Ewing J, Liang X, Lau JT. 2000. Murine B cell differentiation is accompanied by programmed expression of multiple novel beta-galactoside alpha2, 6-sialyltransferase mRNA forms. *Glycobiology.* 10:67–75.

Yan R, Bienkowski MJ, Shuck ME, Miao H, Tory MC, Pauley AM, Brashier JR, Stratman NC, Mathews WR, Buhl AE, et al. 1999. Membrane-anchored aspartyl protease with Alzheimer's disease beta-secretase activity. *Nature.* 402:533–537.

Zhao J, Fu Y, Yasvoina M, Shao P, Hitt B, O'Connor T, Logan S, Maus E, Citron M, Berry R, et al. 2007. Beta-site amyloid precursor protein cleaving enzyme 1 levels become elevated in neurons around amyloid plaques: Implications for Alzheimer's disease pathogenesis. *J Neurosci.* 27:3639–3649.

Glycobiology vol. 19 no. 2 pp. 135–143, 2009
doi:10.1093/glycob/cwn115
Advance Access publication on October 25, 2008

Capillary electrophoresis-electrospray ionization mass spectrometry for rapid and sensitive *N*-glycan analysis of glycoproteins as 9-fluorenylmethyl derivatives

Miyako Nakano[2], Daisuke Higo[3], Etsuo Arai[4], Takatoshi Nakagawa[5], Kazuaki Kakehi[6], Naoyuki Taniguchi[2], and Akihiro Kondo[1,7]

[2]Department of Chemistry and Biomolecular Science, Macquarie University, Sydney NSW 2109, Australia; [3]Bruker Daltonics K. K., 9-A-6F, Moriya 3, Kanagawa-ku, Yokohama 221-0022; [4]Bechman Coulter K. K., 3-5-1, Toranomon, Minato-ku, Tokyo 105-0001; [5]Department of Glycotherapeutics, Osaka University Graduate School of Medicine, Osaka 565-0871, Japan; [6]Faculty of Pharmaceutical Sciences, Kinki University, 3-4-1 Kowakae, Higashi-Osaka 577-8502; and [7]Department of Glycotherapeutics, Osaka University Graduate School of Medicine, Osaka 565-0871, Japan

Received on May 27, 2008; revised on September 20, 2008; accepted on October 12, 2008

It is well known that most protein therapeutics such as monoclonal antibody pharmaceuticals and other biopharmaceuticals including cancer biomarkers are glycoproteins, and thus the development of high-throughput and sensitive analytical methods for glycans is essential in terms of their determination and quality control. We previously reported a novel alternative labeling method for glycans involving 9-fluorenylmethyl chloroformate (Fmoc-Cl) instead of the conventional reductive amination procedure. The derivatives were analyzed by high-performance liquid chromatography (HPLC) (Kamoda S, Nakano M, Ishikawa R, Suzuki S, Kakehi K. 2005. Rapid and sensitive screening of *N*-glycans as 9-fluorenylmethyl derivatives by high-performance liquid chromatography: A method which can recover free oligosaccharides after analysis. *J Proteome Res.* 4:146–152). This method was rapid and simple; however, it was time-consuming in terms of analysis by HPLC and did not provide so much information such as the detailed structures and mass numbers of glycans. Here we have developed a high-throughput and highly sensitive method. It comprises three steps, i.e., release of glycans, derivatization with Fmoc, and capillary electrophoresis-electrospray ionization mass spectrometry (CE-ESI MS) analysis. We analyzed several glycoproteins such as fetuin, alpha1 acid glycoprotein, IgG, and transferrin in order to validate this method. We were able to analyze the above glycoproteins with the three-step procedure within only 5 h, which provided detailed *N*-glycan patterns. Moreover, the MS/MS analysis allowed identification of the *N*-glycan structures. As novel applications, the method was employed for the analysis of *N*-glycans derived from monoclonal antibody pharmaceuticals and also from alpha-fetoprotein; the latter is known as one of the tumor markers of hepatocellular carcinomas. We were able to easily and rapidly determine the detailed structures of the *N*-glycans. The present method is very useful for the analysis of large numbers of samples such as a routine analysis.

[1]To whom correspondence should be addressed: Tel: +81-6-6878-8161; Fax: +81-6-6878-8162; e-mail: kondoa@sahs.med.osaka-u.ac.jp

Keywords: carbohydrate/CE-ESI MS/Fmoc/glycoprotein/*N*-glycan

Introduction

Analysis of glycans linked to proteins is important for precise understanding of the functions of glycoproteins. In contrast to profiling of total proteins (i.e., proteomics), high-throughput analysis of total glycans (i.e., glycomics) is still at a developmental stage, and various techniques for glycan mapping involving high-performance liquid chromatography (HPLC) (Hase and Ikenaka 1990; Takahashi et al. 1993, 1995; Hase 1994; Kondo et al. 1994; Anumula and Dhume 1998; Nakano et al. 2004) and capillary electrophoresis (CE) (Kinoshita et al. 2000; Kakehi et al. 2001) have been reported. High-pH anion exchange chromatography with pulsed amperometric detection is a powerful tool for the analysis of free glycans (Rice et al. 1992; Nakano et al. 2003). CE is an efficient and versatile method for the separation of complex glycan mixtures obtained from biological sources with high sensitivity. CE for glycan analysis involving various modes of sample separation such as simple zone electrophoresis (Ha et al. 2006; Kamoda and Kakehi 2006) and complex formation with borate ions (Suzuki et al. 2003; Sato et al. 2005; Dang et al. 2006) has been developed.

Mass spectrometry (MS) has become a powerful tool for the detection of glycans and for acquiring structural information on them. Online coupling of CE and MS has been proved to be very useful for glycan analysis (Schmitt-Kopplin and Frommberger 2003; Zamfir and Peter-Katalinic 2004; Zamfir et al. 2004). This technique allows minimum sample handling, which significantly reduces potential sample loss, and mass spectrometry is a powerful tool for the extremely selective and sensitive detection of specific structures of glycans. The application of capillary electrophoresis-electrospray ionization mass spectrometry (CE-ESI MS) and MS/MS to glycoscreening in the biomedical field has recently been highlighted (Sandra et al. 2004; Zamfir and Peter-Katalinic 2004). Bindila et al. (2005) reported the analysis of underivatized *O*-glycosylated sialylated amino acid derived from Schindler's disease type I by sheathless reverse-polarity CE-ESI MS. Here, we investigated a method for *N*-glycans involving CE-ESI MS. *N*-Glycans are found in the sequence of Asn-X-Ser/Thr of a protein core, where X can be any amino acid except for proline. For the release of *N*-glycans attached to Asn residues through *N*-glycosidic linkages (structure 1 in Figure 1A), digestion with PNGase F (referred to as peptide N^4-(acetyl-β-D-glucosaminyl) asparagine amidase or peptide: *N*-glycanase F; EC 3.5.1.52) is most frequently performed, and the glycans are released as *N*-glycosylamine (structure 2). The *N*-glycosylamine is readily hydrolyzed to a free form (structure 3) under slightly acidic conditions, but is relatively stable under slightly basic conditions. The free form (structure 3) has

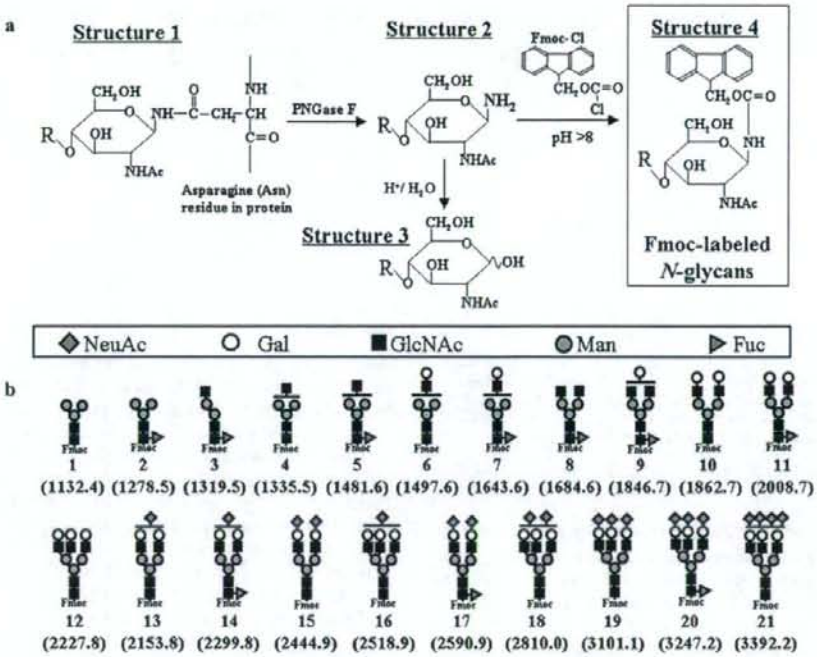

Fig. 1. (**A**) Flowchart for the preparation of Fmoc-labeled *N*-glycans after the release of *N*-glycans from protein. The *N*-glycan (structure 1) linked to the Asn-residue of the core protein/peptide is released with PNGase F as *N*-glycosylamine (structure 2). Structure 2 is hydrolyzed to yield free *N*-glycan (structure 3) under acidic conditions. However, at above pH 8, *N*-glycosylamine (structure 2) can be stabilized, therefore it can be directly reacted the amino groups with Fmoc-Cl. The Fmoc-labeled *N*-glycan (structure 4) was subjected to analysis by CE-ESI MS. (**B**) List of the structures detected in this study. The numbers in parentheses are the mass numbers represented as $[M + H]^+$ of Fmoc-labeled *N*-glycans.

been widely used for the profiling of *N*-glycans after derivatization with fluorogenic and chromophoric reagents such as 2-aminopyridine (PA) and 2-aminobenzamide for HPLC analysis (Hase 1994; Guile et al. 1996), and with 8-aminopyrene-1,3,6-trisulfonate (APTS) (Evangelista et al. 1996; Sei et al. 2002), 2-aminobenzoic acid (2-AA), or 3-aminobenzoic acid (Kakehi et al. 2002) for high-resolution analysis of glycans by CE.

For simpler and more rapid and sensitive analyses, we developed a method for direct labeling of *N*-glycosylamine-type glycans involving 9-fluorenylmethyl chloroformate (Fmoc-Cl) in our previous study (Kamoda et al. 2005) (structures 2 and 4 in Figure 1A). The Fmoc-labeling method has some strong points: (1) simple procedure; Fmoc reagent is just added to the reaction solution after digestion with PNGase F, and it is easy to remove excess reagent by extraction with chloroform, (2) high-speed analysis; within 4 h, including the enzymatic glycan releasing reaction and the labeling reaction before analysis, (3) high-sensitivity; 5 and 30 times higher sensitivities than those for 2-AA and PA-labeled *N*-glycans with a fluorescent detector, respectively, and (4) easy recovery of free-form glycans (structure 3 in Figure 1A); by incubation with morpholine in a dimethylformamide solution at room temperature (Kamoda et al. 2005).

Unlike peptides and proteins, most glycans do not form multiply charged ions; therefore, for the ionization and detection of glycans with large molecular masses, it is generally difficult to obtain good quality data (Macek et al. 2001; Metelmann et al. 2001; Sagi et al. 2002). The CE-ESI MS technique for glycans produces multiply charged ions due to the use of ammonium acetate as the CE buffer (Suzuki-Sawada et al. 1992). Therefore, in the present study, we developed a method for the analysis of Fmoc-labeled *N*-glycans released from glycoproteins involving CE-ESI MS, and the method was applied to the analysis of glycans derived from glycoproteins, such as human α1-acid glycoprotein (AGP), bovine fetuin, human transferrin, and human IgG. Also, we analyzed the *N*-glycans in glycoprotein bands obtained on a sodium dodecyl sulfate–polyacrylamide gel electrophoresis (SDS–PAGE) gel. As applications, this method was applied to the analysis of *N*-glycans derived from some antibody pharmaceuticals and a tumor marker, it being shown that the present technique is a powerful tool for the high-speed screening of *N*-glycans in biological samples.

Results

Release of N-glycans with PNGase F and in situ derivatization with Fmoc

A sample (10 μg) of each of bovine fetuin, human AGP, human transferrin, and human IgG was digested with PNGase F, and the released glycans were derivatized with Fmoc. Bovine fetuin contains monosialo-, disialo-, trisialo-, and tetrasialo-glycans (1SA, 2SA, 3SA, and 4SA, respectively) (Townsend et al. 1986;

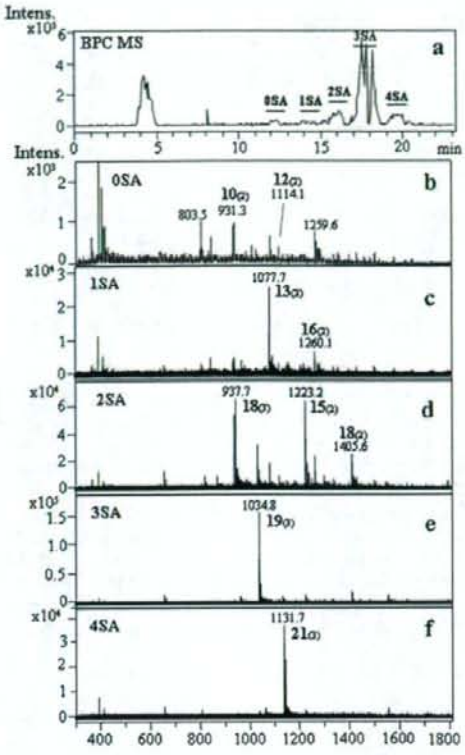

Fig. 2. CE-ESI MS analysis of Fmoc-labeled *N*-glycans from bovine fetuin. (**A**) BPC MS. (**B–F**) The averaged mass spectra of 0SA, 1SA, 2SA, 3SA, and 4SA sections shown in **A**. The structures of *N*-glycans are summarized in Figure 1. The numbers in parentheses are the state of charge ((2) means $[M + 2H]^{2+}$, (3) means $[M + 3H]^{3+}$).

Green et al. 1988). The results of analysis of Fmoc-labeled glycans are shown in Figure 2. In a base peak chromatogram (BPC) on MS (Figure 2A), sialylated *N*-glycans are eluted according to the number of sialic acid residues because of the electroendosmotic flow due to the combination of a bare fused silica capillary with a electrolyte at pH 6.8. Thus, 0SA were observed the earliest at 12 min, and 1SA, 2SA, and 3SA were observed at 14.5, 16, and 18 min, respectively. At about 20 min, 4SA migrated the slowest. It should be noted that CE also facilitated the separation of Fmoc-labeled *N*-glycans from contaminants such as a polymer (the difference between each peak was 135.9 *m/z*) which was detected at around 5 min as a huge peak. The averaged mass spectra of 0SA, 1SA, 2SA, 3SA, and 4SA are shown in Figure 2B–F, respectively. A list of the *N*-glycans observed in the present study is given in Figure 1. The numbers in parentheses under the *N*-glycan structures in Figure 1B are those calculated at the *m/z* of $[M + H]^+$. In Figure 2B, 0SA comprised asialo-biantennary glycan (**10** $[M + 2H]^{2+} = 931.3$ *m/z*) and asialo-triantennary glycan (**12** $[M + 2H]^{2+} = 1114.1$ *m/z*). In Figure 2C, 1SA comprised monosialo-biantennary glycan (**13** $[M + 2H]^{2+} = 1077.7$ *m/z*) and monosialo-triantennary glycan (**16** $[M + 2H]^{2+} = 1260.1$ *m/z*). In Figure 2D, 2SA comprised disialo-biantennary glycan (**15** $[M + 2H]^{2+} = 1223.2$ *m/z*) and disialo-triantennary glycan (**18** $[M + 2H]^{2+} = 1405.6$ *m/z* and $[M + 3H]^{3+} = 937.7$ *m/z*). In Figure 2E and F, 3SA and 4SA comprised trisialo-triantennary glycan (**19** $[M + 3H]^{3+} = 1034.8$ *m/z*) and tetrasialo-triantennary glycan (**21** $[M + 3H]^{3+} = 1131.7$ *m/z*), respectively. From the results of analysis of *N*-glycans derived from bovine fetuin, the peak areas on BPC of the 0SA–4SA *N*-glycans, as shown in Figure 2A, were calculated, and the results were compared with those for the peak areas of the fluorescence intensities determined on HPLC analysis in the previous study (Kamoda et al. 2005). The percentages of the peak areas in the HPLC chromatograms of the 0SA–4SA were 1.1, 3.2, 24.8, 59.4, and 11.5%, respectively, on the other hand, the percentages of peak areas on BPC in the present study were 2.9, 3.5, 14.6, 67.4, and 11.7%. The percentages were, thus, demonstrated to show a similar pattern, therefore, it is possible to determine the amounts of *N*-glycans using this method.

Typical MS/MS spectra of the trisialo-triantennary glycan (**19**) are shown in Figure 3. The fragment ions that released *N*-acetylneuraminic acid (NeuAc), galactose (Gal), *N*-acetylglucosamine (GlcNAc), and mannose (Man) from the nonreducing end, which had Fmoc residues, were observed as singly or doubly charged ones. The ions which did not contain Fmoc residues were observed in the low mass region as singly charged ones. It should be noted that the fragment ion at *m/z* 366 due to lactosamine (Gal-GlcNAc) and that at *m/z* 657 due to sialo-lactosamine (NeuAc-Gal-GlcNAc) were characteristic of complex-type *N*-glycans. We detected all *N*-glycans derived from bovine fetuin that were reported previously (Townsend et al. 1986; Green et al. 1988). We next analyzed *N*-glycans derived from human AGP (Nakano et al. 2004), transferrin (Spik et al. 1975; Satomi et al. 2004), and IgG (Tai et al. 1975; Mizuochi et al. 1982; Takahashi et al. 1987), their *N*-glycans being observed in the order of the number of sialic acid residues (shown in supplementary Figures S1 and S2). We also performed MS/MS analysis, and two typical MS/MS results for *N*-glycans of AGP are shown in supplementary Figure S1. We could identify all the structures that some groups had reported previously.

Analysis of N-glycans in glycoprotein bands obtained on a SDS–PAGE gel

We next examined whether the Fmoc-labeling method was applicable to the direct derivatization of the *N*-glycans released from proteins on SDS–PAGE. Ten micrograms of each of bovine fetuin, human AGP, human transferrin, and human IgG was subjected to SDS–PAGE, followed by staining with Coomassie blue R-250 (CBB). The bands stained with CBB were cut out and destained, and then the materials were digested with PNGase F, derivatized with Fmoc, and then analyzed by CE-ESI MS. The results for bovine fetuin are shown in Figure 4. Fmoc-labeled *N*-glycans were not separated based on the number of sialic acids, and a clear peak of Fmoc-labeled *N*-glycans was not observed on BPC MS (Figure 4A). The reasons were that the yield of *N*-glycans released from the gel was not high, and the contaminating polymer was increased compared with analysis involving in situ digestion. Therefore, the *N*-glycans gave a diffused pattern on electrophoresis on a capillary, and all *N*-glycans were detected widely. However, the averaged mass spectra from 12 to 17 min revealed all *N*-glycan peaks derived

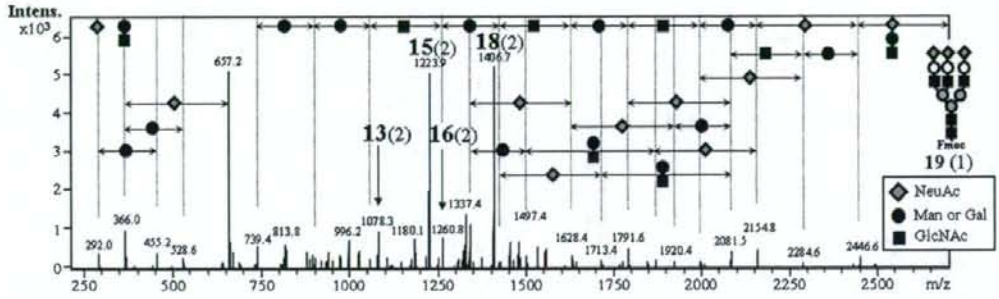

Fig. 3. MS/MS analysis of trisialo-triantennary glycan (19) derived from bovine fetuin shown in Figure 2E. The structures of *N*-glycans are summarized in Figure 1. The numbers in parentheses are the state of charge ((1) means $[M + H]^+$, (2) means $[M + 2H]^{2+}$).

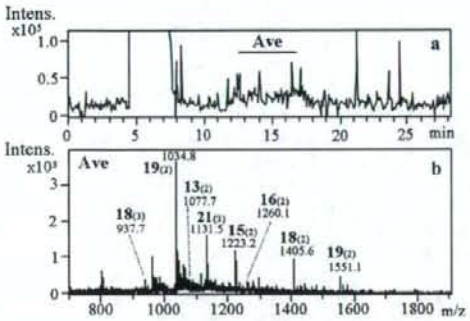

Fig. 4. CE-ESI MS analysis of *N*-glycans derived from bovine fetuin observed on SDS–PAGE gel using the Fmoc-labeling method. (**A**) BPC MS. (**B**) The averaged mass spectra of the section from 12 to 17 min in **A**. The structures of *N*-glycans are summarized in Figure 1.

from bovine fetuin, as shown in Figure 4B. Monosialo-, disialo-, trisialo-, and tetrasialo-triantennary glycans (**16**, **18**, **19**, and **21**) were observed as doubly or triply charged ions. Monosialo- and disialo-biantennary glycans (**13** and **15**) were also observed as doubly charged ions. Regarding the results for human AGP, transferrin and IgG, all *N*-glycans observed on solution phase digestion were observed. Therefore, our results show that the present method is useful for evaluation of the *N*-glycan profiles of glycoproteins after SDS–PAGE separation.

Analysis of N-glycans derived from antibody pharmaceutical preparations

N-Glycans in glycoprotein pharmaceuticals play important roles in the expression of their biological activities. Therefore, the development of an assessment method for these glycans is important for the quality control of glycoprotein pharmaceuticals such as newly developed therapeutic antibodies. The relationship between the biological functions and glycans of antibody pharmaceuticals has been extensively studied. Kumpel et al. reported that the lactosamine structure (i.e., the presence of Gal residues in the nonreducing terminals) affects antibody-dependent cellular cytotoxicity (ADCC), which is a major function of some therapeutic antibodies (Kumpel et al. 1994, 1995). The presence of bisecting GlcNAc has also been reported to improve ADCC (Umana et al. 1999; Davies et al. 2001). Furthermore, recent reports indicated that the absence of a fucose (Fuc) residue at the innermost GlcNAc of reducing ends caused more obvious ADCC than that caused by the presence of bisecting GlcNAc (Shields et al. 2002; Shinkawa et al. 2003). The conditions for the industrial production of glycoprotein pharmaceuticals are quite important for maintaining the consistency of glycans (Parekh et al. 1989; Gawlitzek et al. 1995). Therefore, assessment studies on glycans in glycoprotein pharmaceuticals are crucial for quality assurance. Regulatory agencies are increasingly requiring the determination of glycan distributions quantitatively.

In this study, we applied the combination of Fmoc-labeling and the CE-ESI MS method for the glycan mapping of commercial therapeutic antibody pharmaceuticals: a humanized monoclonal antibody for treating metastatic breast cancer (trastuzumab), a chimeric monoclonal antibody for treating non-Hodgkin's lymphoma (rituximab), and a humanized monoclonal antibody against a respiratory syncytial virus (palivizumab).

The results of analysis of trastuzumab are shown in Figure 5A and B. *N*-Glycans were observed at 8–10 min on BPC MS, as shown in Figure 5A. The result of averaging of the mass spectra (8–10 min) in Figure 5A is shown in Figure 5B. Alpha 1-6 fucosylated monogalactosyl biantennary glycans (**9**), α1-6 fucosylated agalactosyl biantennary glycans (**8**), and α1-6 fucosylated monoGlcNAc biantennary glycans (**5**) were observed as major peaks. Alpha 1-6 fucosylated biantennary glycans (**11**), α1-6 fucosylated mono GlcNAc monogalactosyl biantennary glycans (**7**), and α1-6 fucosylated core five-structure glycan (**2**) were detected as minor peaks. These results were consistent with a previous report of Kamoda et al., who analyzed *N*-glycans in pharmaceutical preparations by CE (Kamoda et al. 2004, 2005). Moreover, we found *N*-glycans without α1-6 Fuc (**1**, **4**, **6**, **10**) and a linear structure glycan without a six-branch Man chain (**3**). The analysis of *N*-glycans derived from rituximab and palivizumab was performed in the same manner, and the relative abundance of each *N*-glycan structure in each antibody pharmaceutical was calculated based on the signal intensities of the corresponding Fmoc-labeled *N*-glycans obtained on CE-ESI MS analysis. Briefly, the total detected signal intensities of Fmoc-labeled *N*-glycans were set at 100% for each antibody pharmaceutical, and the percentage of each Fmoc-labeled *N*-glycan was calculated. The results are summarized in Figure 5C. The relative abundances of *N*-glycan structures in the

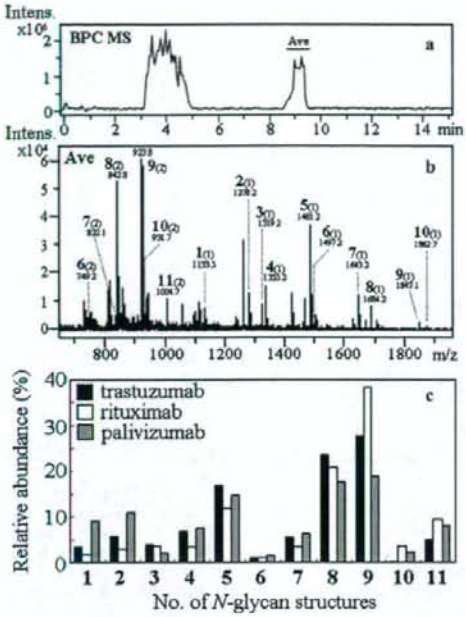

Fig. 5. CE-ESI MS analysis of Fmoc-labeled *N*-glycans released from antibody pharmaceuticals. (**A**) BPC MS of trastuzumab. (**B**) The averaged mass spectra of the section from 8 to 10 min in **A**. (**C**) Relative abundance (%) of *N*-glycans derived from trastuzumab (black bars), rituximab (white bars), and palivizumab (gray bars). The relative abundance was calculated based on the signal intensities of the corresponding Fmoc-labeled *N*-glycans obtained from the results presented in **B**. The structures of *N*-glycans are summarized in Figure 1.

three kinds of antibody pharmaceuticals were basically similar; however, the imperfect structures of *N*-glycans such as (**1**, **2**, **4**) were slightly increased in palivizumab. Trastuzumab and rituximab are produced from CHO cells, and palivizumab is produced from mouse myeloma cells. From these results, we found that the antibody pharmaceuticals from different cells did not show characteristic carbohydrate patterns. This present method is a suitable one for their quality control.

Western blotting and lectin-affinity electrophoresis for α-fetoprotein (AFP), and CE-ESI MS analysis of N-glycans of AFP

Lens culinaris agglutinin (LCA) is a lectin which exhibits affinity to biantennary glycans with α1-6 Fuc (Kaifu et al. 1975). An-reactive AFP with LCA (AFP-L3) has been used as an effective marker for earlier diagnosis, for the assessment of therapeutic effects, and for predicting the prognosis of hepatocellular carcinoma (HCC). Using LCA, AFP is divided into three types as to microheterogeneity (L1, L2, and L3) (Kerckaert et al. 1979). AFP-L1 and L3 are major components of AFP in the serum of HCC patients. This addition of a Fuc residue is mainly observed when there is a structural change in *N*-glycans caused by HCC; therefore, AFP-L3 is highly specific to HCC (Sato et al. 1993; Taketa et al. 1993; Shiraki et al. 1995). In this study, we analyzed *N*-glycans in AFP derived from human normal placenta and human hepatoma cells (Huh-7) in order to determine any differences in *N*-glycan structures for an application for this CE-ESI MS technique. A portion of them was subjected to SDS–PAGE, and only one band was stained with CBB (Figure 6A). The molecular weight corresponding to the band (ca. 75 kDa) was the expected molecular weight of AFP; furthermore, Western blot analysis with anti-AFP antibodies showed that the band was AFP (Figure 6B). Although there was no difference between AFP derived from normal human placenta and Huh-7 cells on both SDS–PAGE analysis and Western blot analysis, there was a big difference on electrophoresis with LCA (Figure 6C). AFP derived from normal human placenta gave one band at the L1 position. AFP derived from Huh-7 cells gave two bands at the L1 and L3 positions. The L3 band means AFP bound to LCA strongly; in other words, AFP at the L3 position has an *N*-glycan containing α1-6 Fuc at the reducing terminus of GlcNAc. We could confirm that nonfucosylated *N*-glycans were major in AFP from normal human placenta, but α1-6 fucosylated *N*-glycans were major in AFP from Huh-7 cells. We next tried to analyze *N*-glycans in these AFPs by means of our CE-ESI MS technique. The results are shown in Figure 6D–J. The *N*-glycans in AFP derived from human normal placenta were observed at 17–19 min (1SA) and 20–21 min (2SA), as shown in Figure 6D (BPC MS). On the other hand, *N*-glycans in AFP derived from Huh-7 cells were observed at 19–20 min (1SA), 21–23 min (2SA), and 24–26 min (3SA), as shown in Figure 6E (BPC MS). *N*-Glycans of 1SA and 2SA from AFP derived from human normal placenta were monosialo biantennary ones (**13** in Figure 6F) and disialo-biantennary ones (**15** in Figure 6G), respectively. We could slightly detect α1-6 fucosylated monosialo- and disialo-biantennary glycans (**14** in Figure 6F and **17** in Figure 6G). These fucocylated *N*-glycans must be included in the L3 fraction in lane p, Figure 6C. On the other hand, the *N*-glycans of 1SA, 2SA, and 3SA from AFP derived from Huh-7 cells were α1-6 fucosylated monosialo-biantennary ones (**14** in Figure 6H), α1-6 fucosylated disialo-biantennary ones (**17** in Figure 6I), and α1-6 fucosylated trisialo-triantennary ones (**20** in Figure 6J), respectively. Disialo-biantennary glycan without Fuc (**15** in Figure 6I) was also slightly detected. This *N*-glycan (**15**) is located at the L1 position in lane h, Figure 6C. From these results, although the electrophoresis with LCA in Figure 6C could reveal differences in the patterns of *N*-glycans in AFP derived from human placenta and Huh-7 cells, our CE-ESI MS technique could reveal the differences based on the detailed *N*-glycan structures.

Discussion

We have developed a simple, rapid and sensitive method involving CE-ESI MS with Fmoc-labeling of *N*-glycans derived from several glycoproteins. We could also identify the *N*-glycans, especially *N*-glycans containing sialic acids, based on the mass number and the fragment pattern on MS/MS analysis with appropriate separation on CE. The advantages of the present CE/MS approach are as follows: (1) *N*-glycans derivatized with fluorogenic or chromophoric reagents such as Fmoc are suitable for detailed MS/MS analysis to investigate the linkage patterns of *N*-glycans. (2) Also, they have a single configuration (i.e., β-form) at the reducing end and have no isomers which

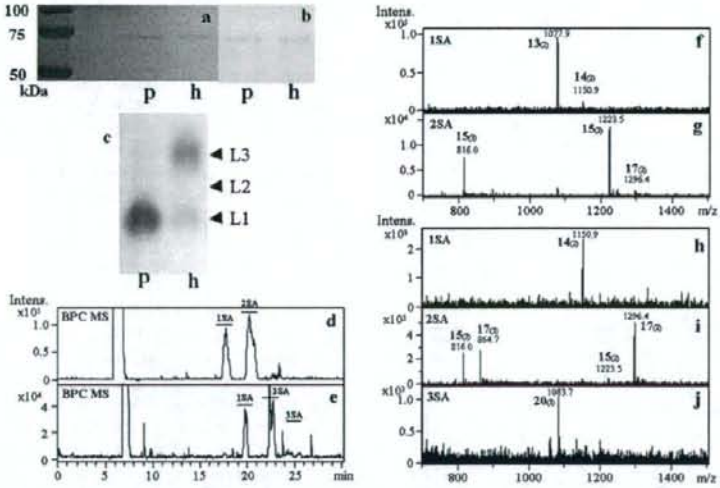

Fig. 6. CE-ESI MS analysis of Fmoc-labeled *N*-glycans derived from AFP. (**A**) SDS–PAGE (12%) analysis of AFP derived from human normal placenta (100 ng, lane p) and Huh-7 cells (100 ng, lane h), followed by CBB staining. (**B**) Western blot analysis using anti-AFP antibodies for AFP derived from human normal placenta (1 ng, lane p) and Huh-7 cells (1 ng, lane h). (**C**) Lectin (LCA)-affinity electrophoresis for AFP derived from human normal placenta (300 ng, lane p) and Huh-7 cells (100 ng, lane h). (**D**) BPC MS of Fmoc-labeled *N*-glycans in AFP derived from human normal placenta. (**E**) BPC MS of Fmoc-labeled *N*-glycans in AFP derived from Huh-7 cells. (**F** and **G**) The averaged mass spectra of the 1SA and 2SA sections in **D**. (**H**–**J**) The averaged mass spectra of the 1SA, 2SA, and 3SA sections in **E**. The structures of *N*-glycans are summarized in Figure 1.

complicate the chromatography. (3) The Fmoc-labeling method is very simple because the releasing of *N*-linked oligosaccharides from a glycoprotein sample followed by labeling with Fmoc is performed in a one-pot reaction. After PNGase F digestion and then Fmoc derivatization, the proteins devoid of *N*-glycans are easily removed as fluffy material during extraction of the excess Fmoc reagent with chloroform (Kamoda et al. 2005). Most recently, Ruhaak et al. (2008) reported a high-throughput method with which *N*-glycans derived from total human plasma glycoproteins were derivatized with 2-AA in a 96-well plate followed by analysis by CE-ESI-Q- TOF-MS. Gennaro et al. also reported a method with which *N*-glycans derived from therapeutic antibodies were derivatized with APTS followed by analysis involving CE-LIF (laser-induced fluorescence)-TOF-MS (Gennaro and Salas-Solano 2008). In both of them, solid-phase extraction is performed to remove excess labeling reagent. In our present method, liquid-phase extraction is performed for this. It is much simpler. (4) Therefore, the method allows rapid mapping of *N*-glycans within 5 h, including an enzymatic glycan releasing reaction, Fmoc derivatization, analysis by CE-ESI MS, and data analysis. (5) The CE separation of *N*-glycans before subjecting them to MS is helpful for identifying the *N*-glycans because *N*-glycans are separated from contaminants such as polymers on a fused silica capillary on CE and then sialo *N*-glycans are eluted in the order of the number of sialic acids in glycans. (6) The ammonium acetate used as the CE buffer facilitates the production of multiple charged ions of labeled *N*-glycans (Suzuki-Sawada et al. 1992), and therefore for the ionization and detection of glycans with large molecular masses, it is easy to obtain good quality data.

We applied this simple, rapid and sensitive method to identify the *N*-glycans released from the bands observed on SDS–PAGE after in-gel digestion. We could directly release *N*-glycans from glycoproteins in a gel without extracting them from the gel. The released *N*-glycans were derivatized with Fmoc followed by CE-ESI MS analysis. The present method is applicable for the analysis of crude samples after separation on a 2D-gel. Hereafter, the rapid analysis of *N*-glycans will be useful for routine work for validation of glycoprotein pharmaceuticals and disease biomarkers. We applied the method to the analysis of *N*-glycans derived from some antibody pharmaceuticals prepared from different kinds of cells and showed the similar characteristic patterns of glycans. We were also able to easily and rapidly determine the *N*-glycan structures of AFP of different sources with various sialylation and fucosylation patterns. In conclusion, this method is a powerful tool for high-speed screening of *N*-glycans in biological samples.

Material and methods

Reagents and materials

PNGase F (EC 3.5.1.52, recombinant) was obtained from Roche Diagnostics (Mannheim, Germany). Fmoc-Cl was from Tokyo Kasei (Tokyo, Japan). Human AGP, bovine fetuin, human transferrin, human IgG, and mouse anti-human AFP monoclonal antibodies were purchased from Sigma (St. Louis, MO). The recombinant antibody pharmaceutical preparations (rIgG), trastuzumab, rituximab, and palivizumab were kindly donated by Ms. Nishiura of Kinki University Nara Hospital. AFP derived from human placenta was purchased from Cosmobio (Tokyo, Japan). Another type of AFP was purified from the conditioned medium of Huh-7 cells (Japanese Collection of Research Bioresources) using an antibody column of polyclonal rabbit

anti-human AFP antibodies. Other reagents and solvents were of HPLC or LC/MS grade.

Release of N-glycans with PNGase F and in situ derivatization with Fmoc

The release of *N*-glycans from several glycoprotein samples and labeling of the *N*-glycosylamine-type glycans with Fmoc were performed according to the procedures reported previously (Kamoda et al. 2005). Glycoprotein samples (10 μg each) were each dissolved in a 20 mM phosphate buffer (pH 8.5, 100 μL) in a sample tube (1.5 mL). PNGase F (1 unit, 1 μL) was added, and the mixture was incubated at 37°C for 2 h. After dilution of the mixture with water (300 μL), a freshly prepared solution (200 μL) of Fmoc-Cl in acetone (50 mg/mL) was added and the mixture was incubated at 37°C for 1 h. Chloroform (300 μL) was added to the mixture, and the mixture was shaken vigorously. After centrifugation, the aqueous layer was transferred to a new sample tube (1.5 mL). Care should be taken not to transfer the fluffy material over the organic layer. Another portion of chloroform (300 μL) was added to the aqueous layer, and the mixture was shaken vigorously to remove the excess reagent. The same procedures for washing the aqueous layer with chloroform were repeated five times. Finally, a portion (5 μL) of the aqueous layer containing *N*-glycans derivatized with Fmoc was transferred to a sample vial for injection into the CE-ESI MS. The workflow for this procedure is shown by a run in supplementary Figure S3.

Analysis of N-glycans in glycoprotein bands obtained on a SDS–PAGE gel

A 10 μg aliquot of each of bovine fetuin, human AGP, transferrin, and IgG was subjected to SDS–PAGE (acrylamide 12%) followed by staining with CBB. The glycoprotein band visualized with CBB was rinsed with distilled water in a sample tube and then cut into small pieces (1 mm^2). The gel pieces were rinsed with an aqueous solution (500 μL) of 50 mM ammonium bicarbonate in 30% acetonitrile for 10 min to remove the dye reagent. This procedure was repeated three times. The gel pieces were kept in acetonitrile (500 μL) for 10 min for dehydration. The acetonitrile was removed and the gel pieces were dried for 15 min under reduced pressure. PNGase F (1 U) in the 20 mM phosphate buffer (pH 8.5, 5 μL) was added to the dried gel pieces. After the gel pieces had been swollen, the 20 mM phosphate buffer (pH 8.5, 95 μL) was added and the mixture was incubated at 37°C overnight. After dilution of the mixture with water (300 μL), a freshly prepared solution of Fmoc-Cl in acetone (200 μL, 50 mg/mL) was added, and then the mixture was incubated at 37°C for 1 h. After removing the excess Fmoc reagent with chloroform as described above, the aqueous layer was evaporated to dryness with a centrifugal evaporator. The residue was dissolved in water (20 μL), and a portion (5 μL) was employed for CE-ESI MS analysis. The workflow for this procedure is shown by a run in supplementary Figure S3.

Analysis of N-glycans derived from antibody pharmaceutical preparations

Aqueous solutions of pharmaceutical preparations (trastuzumab, rituximab, and palivizumab) were dialyzed against distilled water for 3 days, the water being changed several times at 4°C using cellulose membrane tubing (Sanko Junyaku, Tokyo, Japan), and then freeze-dried. Each freeze-dried pharmaceutical preparation (10 μg) was dissolved in the 20 mM phosphate buffer (pH 8.5, 100 μL). The following procedure was the same as that described above.

Western blotting and lectin-affinity electrophoresis for AFP, and CE-ESI MS analysis of N-glycans of AFP

AFP derived from human placenta and Huh-7 cells (100 ng each) was subjected to SDS–PAGE (10% (w/v) polyacrylamide) followed by staining with Coomassie blue R-250. For Western blotting, AFP derived from human placenta and Huh-7 (1 ng each) was subjected to SDS–PAGE (10% (w/v) polyacrylamide). We also performed lectin-affinity electrophoresis to examine the *N*-glycan structures of AFP using an AFP differentiation kit L (Wako Pure Chemical Industries, Osaka, Japan). For better understanding of the results of lectin-affinity electrophoresis, the *N*-glycan profile of AFP on CE-ESI MS was examined as follows. *N*-Glycans were released with PNGase F as described above after denaturing the protein with RapiGest SF (Waters, Milford, MA). Briefly, a sample of AFP (10 μg) was dissolved in the 20 mM phosphate buffer (pH 8.5, 90 μL) in a sample tube (1.5 mL). RapiGest SF (10 μL) in the 20 mM phosphate buffer (pH 8.5, 1%) was added, and the mixture was incubated at 60°C for 1 h. After the sample had been cooled to room temperature, PNGase F (1 unit, 1 μL) was added, and then the mixture was incubated at 37°C for 2 h. The derivatization of the released *N*-glycans with Fmoc and removal of the excess Fmoc reagent with chloroform were performed in the same manners as described above. Also, the aqueous layer was evaporated to dryness in a centrifugal evaporator. The residue was dissolved in water (20 μL), and a portion was employed for CE-ESI MS analysis.

CE-ESI MS

CE was performed using a Beckman P/ACE MDQ system (Beckman, Fullerton, CA). The system was online coupled to an Esquire HCT ion trap mass spectrometer (Bruker Daltonics, Germany) via a capillary and a sprayer device (Bruker Daltonics). The capillary was positioned at an orthogonal position as to the ion source. The capillary inlet was placed in a vial containing the CE buffer (50 mM ammonium acetate) and a platinum electrode connected to a high-voltage power supply. All experiments were performed using an eCAP fused silica capillary (Beckman, 100 cm × 50 μm I.D., 360 μm O.D.) installed in an eCAP user-assembled capillary cartridge EDA (Beckman). The capillary had previously been washed with methanol (3 min, 50 psi) and water (2 min, 50 psi), followed by reconditioning with 0.1 M NaOH (2 min, 50 psi) and water (2 min, 50 psi) by means of the pressure method. Finally, the CE buffer was introduced into the capillary (4 min, 50 psi). The capillary was rinsed with the CE buffer (5 min, 50 psi) after each run. A sample solution (Fmoc-labeled *N*-glycans in water) was introduced into the capillary by means of the pressure method (15 s, 3 psi), and then analyzed at the applied potential of 30 kV at 20°C. The sample solution reaching the outlet of the capillary was sprayed with nebulizing gas (N_2, 8 psi). The sheath liquid comprising 50/49.9/0.1 (v/v/v) MeOH/water/formic acid was delivered to the probe tip at the rate of 2 μL/min. No electrical contact was applied on the outlet of the capillary. The sheath liquid was supplied to maintain a constant flow by means of a syringe pump

(Cole-Parmer, Vernon Hills, IL). In the MS device, the voltage of the capillary outlet was set at −4 kV, and the temperature of the transfer capillary was maintained at 300°C. The flow rate of nitrogen gas for drying was 4 L/min. The MS spectra were obtained in the positive ion mode. The mass range covered was between *m/z* 300 and *m/z* 2000. The scan rates were 8100 amu/s for the MS mode and 26,000 amu/s for the MS/MS mode. The analytical conditions and analytical devices used for the present study are illustrated in supplementary Figure S4.

Supplementary data

Supplementary data for this article is available online at http://glycob.oxfordjournals.org/

Funding

A part of this work was supported by the 21st Century Center of Excellence Program of the Ministry of Education, Culture, Sports, Science, and Technology of Japan, the Core Research for Evolutional Science and Technology, the Core to Core Program and Grant-in-Aid for Scientific Research.

Conflict of interest statement

None declared.

Abbreviations

2-AA, 2-aminobenzoic acid; ADCC, antibody-dependent cellular cytotoxicity; AFP, α-fetoprotein; AGP, α1-acid glycoprotein; BPC, base peak chromatogram; CE-ESI MS, capillary electrophoresis-electrospray ionization mass spectrometry; Fmoc-Cl, 9-fluorenylmethyl chloroformate; Fuc, fucose; Gal, galactose; GlcNAc, *N*-acetylglucosamine; HCC, hepatocellular carcinoma; HPLC, high-performance liquid chromatography; LCA, *Lens culinaris* agglutinin; Man, mannose; NeuAc, *N*-acetylneuraminic acid; PA, pyridylamino; SDS–PAGE, sodium dodecyl sulfate–polyacrylamide gel electrophoresis.

References

Anumula KR, Dhume ST. 1998. High resolution and high sensitivity methods for oligosaccharide mapping and characterization by normal phase high performance liquid chromatography following derivatization with highly fluorescent anthranilic acid. *Glycobiology.* 8:685–694.

Bindila L, Peter-Katalinic J, Zamfir A. 2005. Sheathless reverse-polarity capillary electrophoresis-electrospray-mass spectrometry for analysis of underivatized glycoconjugates. *Electrophoresis.* 26:1488–1499.

Dang F, Kakehi K, Nakajima K, Shinohara Y, Ishikawa M, Kaji N, Tokeshi M, Baba Y. 2006. Rapid analysis of oligosaccharides derived from glycoproteins by microchip electrophoresis. *J Chromatogr A.* 1109:138–143.

Davies J, Jiang L, Pan LZ, LaBarre MJ, Anderson D, Reff M. 2001. Expression of GnTIII in a recombinant anti-CD20 CHO production cell line: Expression of antibodies with altered glycoforms leads to an increase in ADCC through higher affinity for FC gamma RIII. *Biotechnol Bioeng.* 74:288–294.

Evangelista RA, Liu MS, Rampal S, Chen FT. 1996. Characterization of fluorescent nucleoside triphosphates by capillary electrophoresis with laser-induced fluorescence detection: Action of alkaline phosphatase and DNA polymerase. *Anal Biochem.* 235:89–97.

Gawlitzek M, Valley U, Nimtz M, Wagner R, Conradt HS. 1995. Characterization of changes in the glycosylation pattern of recombinant proteins from BHK-21 cells due to different culture conditions. *J Biotechnol.* 42:117–131.

Gennaro LA, Salas-Solano O. 2008. Online CE-LIF-MS technology for the direct characterization of *N*-linked glycans from therapeutic antibodies. *Anal Chem.* 80:3838–3845.

Green ED, Adelt G, Baenziger JU, Wilson S, Van Halbeek H. 1988. The asparagine-linked oligosaccharides on bovine fetuin. Structural analysis of *N*-glycanase-released oligosaccharides by 500-megahertz 1H NMR spectroscopy. *J Biol Chem.* 263:18253–18268.

Guile GR, Rudd PM, Wing DR, Prime SB, Dwek RA. 1996. A rapid high-resolution high-performance liquid chromatographic method for separating glycan mixtures and analyzing oligosaccharide profiles. *Anal Biochem.* 240:210–226.

Ha PT, Hoogmartens J, Van Schepdael A. 2006. Recent advances in pharmaceutical applications of chiral capillary electrophoresis. *J Pharm Biomed Anal.* 41:1–11.

Hase S. 1994. High-performance liquid chromatography of pyridylaminated saccharides. *Methods Enzymol.* 230:225–237.

Hase S, Ikenaka T. 1990. Estimation of elution times on reverse-phase high-performance liquid chromatography of pyridylamino derivatives of sugar chains from glycoproteins. *Anal Biochem.* 184:135–138.

Kaifu R, Osawa T, Jeanloz RW. 1975. Synthesis of 2-*O*-(2-acetamido-2-deoxy-beta-D-glucopyranosyl)-D-mannose, and its interaction with D-mannose-specific lectins. *Carbohydr Res.* 40:111–117.

Kakehi K, Kinoshita M, Kawakami D, Tanaka J, Sei K, Endo K, Oda Y, Iwaki M, Masuko T. 2001. Capillary electrophoresis of sialic acid-containing glycoprotein. Effect of the heterogeneity of carbohydrate chains on glycoform separation using an alpha1-acid glycoprotein as a model. *Anal Chem.* 73:2640–2647.

Kakehi K, Kinoshita M, Nakano M. 2002. Analysis of glycoproteins and the oligosaccharides thereof by high-performance capillary electrophoresis-significance in regulatory studies on biopharmaceutical products. *Biomed Chromatogr.* 16:103–115.

Kamoda S, Kakehi K. 2006. Capillary electrophoresis for the analysis of glycoprotein pharmaceuticals. *Electrophoresis.* 27:2495–2504.

Kamoda S, Nakano M, Ishikawa R, Suzuki S, Kakehi K. 2005. Rapid and sensitive screening of *N*-glycans as 9-fluorenylmethyl derivatives by high-performance liquid chromatography: A method which can recover free oligosaccharides after analysis. *J Proteome Res.* 4:146–152.

Kamoda S, Nomura C, Kinoshita M, Nishiura S, Ishikawa R, Kakehi K, Kawasaki N, Hayakawa T. 2004. Profiling analysis of oligosaccharides in antibody pharmaceuticals by capillary electrophoresis. *J Chromatogr A.* 1050:211–216.

Kerckaert JP, Bayard B, Biserte G. 1979. Microheterogeneity of rat, mouse and human alpha1-fetoprotein as revealed by polyacrylamide gel electrophoresis and by crossed immuno-affino-electrophoresis with different lectins. *Biochim Biophys Acta.* 576:99–108.

Kinoshita M, Murakami E, Oda Y, Funakubo T, Kawakami D, Kakehi K, Kawasaki N, Morimoto K, Hayakawa T. 2000. Comparative studies on the analysis of glycosylation heterogeneity of sialic acid-containing glycoproteins using capillary electrophoresis. *J Chromatogr A.* 866:261–271.

Kondo A, Kiso M, Hasegawa A, Kato I. 1994. Separation of pyridylamino oligosaccharides by high-performance liquid chromatography on an amine-bearing silica column. *Anal Biochem.* 219:21–25.

Kumpel BM, Rademacher TW, Rook GA, Williams PJ, Wilson IB. 1994. Galactosylation of human IgG monoclonal anti-D produced by EBV-transformed B-lymphoblastoid cell lines is dependent on culture method and affects Fc receptor-mediated functional activity. *Hum Antibodies Hybridomas.* 5:143–151.

Kumpel BM, Wang Y, Griffiths HL, Hadley AG, Rook GA. 1995. The biological activity of human monoclonal IgG anti-D is reduced by beta-galactosidase treatment. *Hum Antibodies Hybridomas.* 6:82–88.

Macek B, Hofsteenge J, Peter-Katalinic J. 2001. Direct determination of glycosylation sites in *O*-fucosylated glycopeptides using nano-electrospray quadrupole time-of-flight mass spectrometry. *Rapid Commun Mass Spectrom.* 15:771–777.

Metelmann W, Peter-Katalinic J, Muthing J. 2001. Gangliosides from human granulocytes: A nano-ESI QTOF mass spectrometry fucosylation study of low abundance species in complex mixtures. *J Am Soc Mass Spectrom.* 12:964–973.

Mizuochi T, Taniguchi T, Shimizu A, Kobata A. 1982. Structural and numerical variations of the carbohydrate moiety of immunoglobulin G. *J Immunol.* 129:2016–2020.

Nakano M, Kakehi K, Lee YC. 2003. Sample clean-up method for analysis of complex-type *N*-glycans released from glycopeptides. *J Chromatogr A.* 1005:13–21.

Nakano M, Kakehi K, Tsai MH, Lee YC. 2004. Detailed structural features of glycan chains derived from alpha1-acid glycoproteins of several different animals: The presence of hypersialylated, *O*-acetylated sialic acids but not disialyl residues. *Glycobiology.* 14:431–441.

Parekh RB, Dwek RA, Thomas JR, Opdenakker G, Rademacher TW, Wittwer AJ, Howard SC, Nelson R, Siegel NR, Jennings MG. 1989. Cell-type-specific and site-specific *N*-glycosylation of type I and type II human tissue plasminogen activator. *Biochemistry.* 28:7644–7662.

Rice KG, Takahashi N, Namiki Y, Tran AD, Lisi PJ, Lee YC. 1992. Quantitative mapping of the *N*-linked sialyloligosaccharides of recombinant erythropoietin: Combination of direct high-performance anion-exchange chromatography and 2-aminopyridine derivatization. *Anal Biochem.* 206:278–287.

Ruhaak LR, Huhn C, Waterreus WJ, de Boer AR, Neususs C, Hokke CH, Deelder AM, Wuhrer M. 2008. Hydrophilic interaction chromatography-based high-throughput sample preparation method for *N*-glycan analysis from total human plasma glycoproteins. *Anal Chem.* 80:6119–6126.

Sagi D, Peter-Katalinic J, Conradt HS, Nimtz M. 2002. Sequencing of tri- and tetraantennary *N*-glycans containing sialic acid by negative mode ESI QTOF tandem MS. *J Am Soc Mass Spectrom.* 13:1138–1148.

Sandra K, Van Beeumen J, Stals I, Sandra P, Claeyssens M, Devreese B. 2004. Characterization of cellobiohydrolase I *N*-glycans and differentiation of their phosphorylated isomers by capillary electrophoresis-Q-Trap mass spectrometry. *Anal Chem.* 76:5878–5886.

Sato K, Sato K, Okubo A, Yamazaki S. 2005. Separation of 2-aminobenzoic acid-derivatized glycosaminoglycans and asparagine-linked glycans by capillary electrophoresis. *Anal Sci.* 21:21–24.

Sato Y, Nakata K, Kato Y, Shima M, Ishii N, Koji T, Taketa K, Endo Y, Nagataki S. 1993. Early recognition of hepatocellular carcinoma based on altered profiles of alpha-fetoprotein. *N Engl J Med.* 328:1802–1806.

Satomi Y, Shimonishi Y, Hase T, Takao T. 2004. Site-specific carbohydrate profiling of human transferrin by nano-flow liquid chromatography/electrospray ionization mass spectrometry. *Rapid Commun Mass Spectrom.* 18:2983–2988.

Schmitt-Kopplin P, Frommberger M. 2003. Capillary electrophoresis-mass spectrometry: 15 years of developments and applications. *Electrophoresis.* 24:3837–3867.

Sei K, Nakano M, Kinoshita M, Masuko T, Kakehi K. 2002. Collection of alpha1-acid glycoprotein molecular species by capillary electrophoresis and the analysis of their molecular masses and carbohydrate chains. Basic studies on the analysis of glycoprotein glycoforms. *J Chromatogr A.* 958:273–281.

Shields RL, Lai J, Keck R, O'Connell LY, Hong K, Meng YG, Weikert SH, Presta LG. 2002. Lack of fucose on human IgG1 *N*-linked oligosaccharide improves binding to human Fcgamma RIII and antibody-dependent cellular toxicity. *J Biol Chem.* 277:26733–26740.

Shinkawa T, Nakamura K, Yamane N, Shoji-Hosaka E, Kanda Y, Sakurada M, Uchida K, Anazawa H, Satoh M, Yamasaki M. 2003. The absence of fucose but not the presence of galactose or bisecting *N*-acetylglucosamine of human IgG1 complex-type oligosaccharides shows the critical role of enhancing antibody-dependent cellular cytotoxicity. *J Biol Chem.* 278:3466–3473.

Shiraki K, Takase K, Tameda Y, Hamada M, Kosaka Y, Nakano T. 1995. A clinical study of lectin-reactive alpha-fetoprotein as an early indicator of hepatocellular carcinoma in the follow-up of cirrhotic patients. *Hepatology.* 22:802–807.

Spik G, Bayard B, Fournet B, Strecker G, Bouquelet S, Montreuil J. 1975. Studies on glycoconjugates: LXIV. Complete structure of two carbohydrate units of human serotransferrin. *FEBS Lett.* 50:296–299.

Suzuki S, Ishida Y, Arai A, Nakanishi H, Honda S. 2003. High-speed electrophoretic analysis of 1-phenyl-3-methyl-5-pyrazolone derivatives of monosaccharides on a quartz microchip with whole-channel UV detection. *Electrophoresis.* 24:3828–3833.

Suzuki-Sawada J, Umeda Y, Kondo A, Kato I. 1992. Analysis of oligosaccharides by on-line high performance liquid chromatography and ion-spray mass spectrometry. *Anal Biochem.* 207:203–207.

Tai T, Ito S, Yamashita K, Muramatsu T, Kobata A. 1975. Asparagine-linked oligosaccharide chains of IgG: A revised structure. *Biochem Biophys Res Commun.* 65:968–974.

Takahashi N, Ishii I, Ishihara H, Mori M, Tejima S, Jefferis R, Endo S, Arata Y. 1987. Comparative structural study of the *N*-linked oligosaccharides of human normal and pathological immunoglobulin G. *Biochemistry.* 26:1137–1144.

Takahashi N, Nakagawa H, Fujikawa K, Kawamura Y, Tomiya N. 1995. Three-dimensional elution mapping of pyridylaminated *N*-linked neutral and sialyl oligosaccharides. *Anal Biochem.* 226:139–146.

Takahashi N, Wada Y, Awaya J, Kurono M, Tomiya N. 1993. Two-dimensional elution map of GalNAc-containing *N*-linked oligosaccharides. *Anal Biochem.* 208:96–109.

Taketa K, Endo Y, Sekiya C, Tanikawa K, Koji T, Taga H, Satomura S, Matsuura S, Kawai T, Hirai H. 1993. A collaborative study for the evaluation of lectin-reactive alpha-fetoproteins in early detection of hepatocellular carcinoma. *Cancer Res.* 53:5419–5423.

Townsend RR, Hardy MR, Wong TC, Lee YC. 1986. Binding of *N*-linked bovine fetuin glycopeptides to isolated rabbit hepatocytes: Gal/GalNAc hepatic lectin discrimination between Gal beta(1,4)GlcNAc and Gal beta(1,3)GlcNAc in a triantennary structure. *Biochemistry.* 25:5716–5725.

Umana P, Jean-Mairet J, Moudry R, Amstutz H, Bailey JE. 1999. Engineered glycoforms of an antineuroblastoma IgG1 with optimized antibody-dependent cellular cytotoxic activity. *Nat Biotechnol.* 17:176–180.

Zamfir A, Peter-Katalinic J. 2004. Capillary electrophoresis-mass spectrometry for glycoscreening in biomedical research. *Electrophoresis.* 25:1949–1963.

Zamfir A, Seidler DG, Schonherr E, Kresse H, Peter-Katalinic J. 2004. On-line sheathless capillary electrophoresis/nanoelectrospray ionization-tandem mass spectrometry for the analysis of glycosaminoglycan oligosaccharides. *Electrophoresis.* 25:2010–2016.

Glycobiology vol. 19 no. 4 pp. 368–374, 2009
doi:10.1093/glycob/cwn145
Advance Access publication on Decmber 18, 2008

Bidirectional *N*-acetylglucosamine transfer mediated by β-1,4-*N*-acetylglucosaminyltransferase III

Takahiro Okada[2,3], Hideyuki Ihara[2], Ritsu Ito[2], Naoyuki Taniguchi[4,5], and Yoshitaka Ikeda[1,2,3]

[2]Division of Molecular Cell Biology, Department of Biomolecular Sciences, Saga University Faculty of Medicine, 5-1-1 Nabeshima, Saga 849-8501, Japan; [3]Core Research for Evolutional Science and Technology (CREST), Japan Science and Technology Agency (JST), 4-1-8 Honcho, Kawaguchi, Saitama 332-0012, Japan; [4]Department of Disease Glycomics, Research Institute for Microbial Diseases, Osaka University, 2-1 Yamadaoka, Suita, Osaka 565-0871, Japan; and [5]Systems and Glycobiology Group, Advanced Research Institute, RIKEN, 2-1 Hirosawa, Wako, Saitama 351-0198, Japan

Received on October 15, 2008; revised on December 4, 2008; accepted on December 8, 2008

β-1,4-*N*-Acetylglucosaminyltransferase III (GnT-III) catalyzes the formation of the bisecting GlcNAc and plays a regulatory role in the biosynthesis of the *N*-linked oligosaccharide. In this study, we examined whether the glycosyl transfer catalyzed by GnT-III is reversible, and, in addition, investigated the equilibrium of the GnT-III-catalyzed reaction. Incubation of the agalactosyl-bisected biantennary oligosaccharide with GnT-III in the presence of the sufficiently high concentration of uridine diphosphate (UDP) resulted in conversion of the bisected oligosaccharide into the nonbisected one. This reaction was accompanied by the stoichiometric formation of UDP-GlcNAc, which appeared to result from the transfer of GlcNAc from the oligosaccharide to UDP. Thus, these results indicate that GnT-III is capable of perceivably catalyzing the reverse reaction in vitro, as found in some glycosyltransferases. When the equilibrium of the reaction was kinetically analyzed, it was found that the state of the equilibrium is greatly displaced toward the formation of the bisecting GlcNAc. In terms of free energy change, as estimated, the reaction by GnT-III can be comparable to the hydrolysis of ATP. Although GnT-III catalyzes bidirectional transfer of GlcNAc between the oligosaccharide and UDP, the removal of the bisecting GlcNAc is unlikely in vivo, due to the displacement of the equilibrium. It is known that equilibria of certain glycosyltransferase reactions are not biased as greatly as the case of GnT-III, and thus it seems likely that there are a variety of equilibrium states in glycosyltransferase reactions. In living cells, the assembly of oligosaccharides could be regulated by not only rate control but also equilibrium control.

Keywords: bidirectional reaction/bisecting GlcNAc/equilibrium/GnT-III/*N*-glycan

[1]To whom correspondence should be addressed: Tel: +81-952-34-2190; Fax: +81-952-34-2189; e-mail: yikeda@med.saga-u.ac.jp

Introduction

Glycosyltransferases are a ubiquitous group of enzymes that catalyze the transfer of carbohydrate moieties from activated nucleotide sugar donors onto a variety of biological molecules, thus contributing to the biosynthesis of oligosaccharides, glycosamininoglycans, and glycoproteins (Sears and Wong 2001; Wacker et al. 2002; Deangelis et al. 2003; Breton et al. 2006). Catalytic mechanisms of glycosyltransferases are becoming clearer by many studies of kinetic and structural analyses (Lairson et al. 2008). In a major class of glycosyltransferases, enzyme carboxylates are required to coordinate a phosphate-bound divalent cation such as manganese or magnesium ions in the interaction with activated sugar donors, and an acid-base catalyst is also required to facilitate nucleophilic attack by the sugar acceptor and elimination of aglycon of the donor (Lairson et al. 2008).

In many studies, enzymatic properties of glycosyltransferases have been examined to investigate the synthetic pathways of glycoconjugates, many of which arise in vivo, and it might have been expediently considered that glycosyltransferases are essentially unidirectional catalysts (Koeller and Wong 2000), possibly in part, due to the undiscoveredness of biological significance of the reverse reaction which may yield a monosaccharide unit-shortened glycoconjugate and a corresponding nucleotide sugar. In some cases, however, it was found that reversibility of glycosyltransferase reactions is evident (Cuypers et al. 1984; Peters et al. 1986; Bulter et al. 1997; Miller et al. 1999). For example, it is well known that sucrose synthase catalyzes the cleavage of sucrose with NDP to fructose and NDP-glucose (Bulter et al. 1997), and a similar reverse reaction was also identified in flavonol 3-*O*-galactosyltransferase (Miller et al. 1999). Recently, mammalian α-2,3-sialyltransferase has been shown to catalyze both forward and reverse reactions at different reaction coordinates as well as some glycosyltransferases used for enzymatic synthesis of anticancer and antibiotic drugs and thereby to enable indirect transglycosylation in which a sugar moiety from one product backbone is transferred to a distinct product scaffold (Minami et al. 2005; Zhang et al. 2006; Chandrasekaran et al. 2008).

UDP-*N*-acetylglucosamine:β-D-mannoside β-1,4-*N*-acetylglucosaminyltransferase III (GnT-III, EC 2.4.1.144) is a mammalian Golgi-resident glycosyltransferase and catalyzes the attachment of the bisecting GlcNAc residue to β-1,4 mannose in the core structure of *N*-linked oligosaccharides (Narashimhan 1982; Nishikawa et al. 1992). The introduction of the bisecting GlcNAc is known to prevent the actions of α-mannosidase II, *N*-acetylglucosaminyltransferases II, IV, and V, and core α-1,6-fucosyltransferase, therefore inhibiting the formation of further branches and core fucosylation (Narashimhan 1982; Gleeson and Schachter 1983;

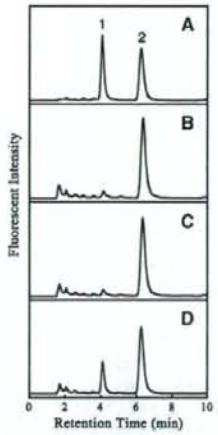

Fig. 1. Conversion of the bisected biantennary oligosaccharide catalyzed by GnT-III. The bisected biantennary oligosaccharide was incubated with UDP (**B**), purified recombinant GnT-III (**C**), and both UDP and purified recombinant GnT-III (**D**), respectively. Standard oligosaccharides (**A**) and reaction products were separated by reversed-phase HPLC. Numbers at the top represent the elution points for the oligosaccharides: 1, biantennary; 2, bisected biantennary.

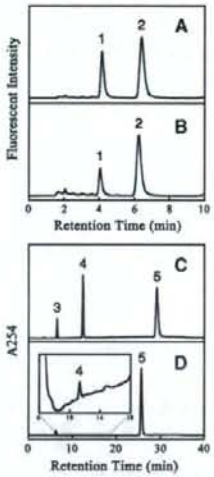

Fig. 2. HPLC profiles of the products of the GnT-III reverse reaction. The purified recombinant GnT-III was incubated with the bisected biantennary oligosaccharide and 100 mM UDP at 37°C. The reaction mixture was boiled and analyzed by reversed-phase HPLC (**B**) and anion-exchange HPLC (**D**). Standard oligosaccharides and UMP/UDP/UDP-GlcNAc were separated by reversed-phase HPLC (**A**) and anion-exchange HPLC (**C**), respectively. The experimental conditions are described under "Materials and methods". Numbers at the top represent the elution points for the products: 1, biantennary oligosaccharide; 2, bisected biantennary oligosaccharide; 3, UMP; 4, UDP-GlcNAc; 5, UDP.

Schachter et al. 1983; Allen et al. 1984; Bendiak and Schachter 1987; Brockhausen et al. 1988; Nishikawa et al. 1992) and also partially inhibits galactosylation by β-1,4-galactosyltransferase (Schachter 1986; Koyota et al. 2001). As suggested by these observations, it has been believed that the prior action of GnT-III is closely related to the regulation of the biosynthesis of complex and hybrid types of the *N*-linked oligosaccharide.

Because regulatory roles of GnT-III in the biosyntheses of *N*-linked oligosaccharides are based essentially on the formation of the bisecting GlcNAc, reversal of the addition of the bisecting GlcNAc by GnT-III may lead to more complicated regulation than believed to date. Thus, it would be desired to examine whether the enzyme is capable of perceivably catalyzing the reverse reaction in order to provide an insight into the GnT-III-conducted regulation. In this study, we investigate the reverse reaction catalyzed by GnT-III in order to examine whether such a reaction is likely to occur in vivo or not.

Results

Removal of the bisecting GlcNAc catalyzed by GnT-III

In order to examine whether GnT-III catalyzes the removal of the bisecting GlcNAc residue from an oligosaccharide substrate, the purified GnT-III which was produced by the baculovirus-insect cell expression system was incubated at 37°C with pyridylaminated (PA)-agalactosyl-bisected biantennary in the presence of UDP and manganese ion. As shown in Figure 1D, it was found that the bisected oligosaccharide was converted to the nonbisected. Mass spectrometric analysis revealed the loss of one GlcNAc residue from the bisected biantennary (data not shown). The resulting oligosaccharide product was also confirmed to act as an acceptor substrate for the addition of the bisecting GlcNAc by GnT-III with UDP-GlcNAc. When the reaction was carried out in the absence of either of UDP or the enzyme, no conversion was observed (Figure 1B and C). Incubation of the oligosaccharide with only the enzyme led to no loss of the bisected oligosaccharide (Figure 1C), indicating that this removal of the bisecting GlcNAc is not due to possible contamination of glycosidase. In fact, the reaction with both GnT-III and UDP did not produce any other oligosaccharide species that lacked either or both of GlcNAc residues linked to two α-mannoses. It was also verified that no removal of the bisecting GlcNAc in Figure 1C is not due to low ionic strength. These results indicate that GnT-III catalyzes the removal of the bisecting GlcNAc from the bisected oligosaccharide, producing the corresponding nonbisected sugar chain.

Stoichiometric formation of the reaction products, UDP-GlcNAc, and nonbisected oligosaccharide

As described above, it was found that GnT-III is capable of removing the bisecting GlcNAc residue, but it was not known whether the nonbisected oligosaccharide product was formed by the glycosyltransferase activity catalyzing a reverse reaction. Otherwise, it could also be due to the possible glycosidase-like activity of the glycosyltransferase. To verify that the removal of the bisecting GlcNAc is due to the transfer of the sugar to UDP, we examined UDP-GlcNAc production accompanying the formation of the nonbisected oligosaccharide (Figure 2). Anion-exchange chromatography performed on a high-performance liquid chromatography (HPLC) system was used to assay UDP-GlcNAc discriminating UDP. The anion-exchange HPLC successfully separated a small amount of UDP-GlcNAc and excess

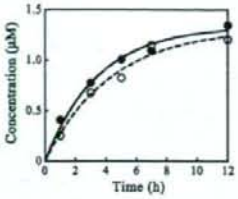

Fig. 3. Time-dependent increase in GnT-III reverse reaction products. The purified recombinant GnT-III was incubated with the bisected biantennary oligosaccharide and 100 mM UDP at 37°C. The reaction mixture was assayed at different times, and the resulting products were monitored by reversed-phase and anion-exchange HPLC analysis. Closed circle denotes the biantennary oligosaccharide and opened circle denotes UDP-GlcNAc.

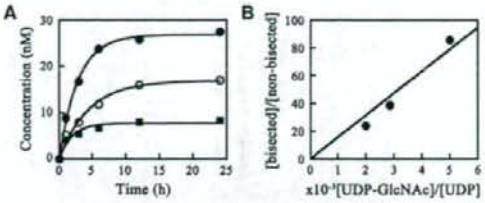

Fig. 4. Equilibrium of the GnT-III-mediated bidirectional reaction under various concentrations of UDP. The purified recombinant GnT-III was incubated with the bisected biantennary oligosaccharide, 2 μM UDP-GlcNAc, and 40–100 mM UDP at 37°C. At different times, the reaction mixture was collected and the biantennary oligosaccharide was quantified by reversed-phase HPLC analysis. (**A**) Time course of the conversion of the bisected oligosaccharide into the nonbisected. Closed square, opened circle, and closed circle denote that UDP concentrations were 40 mM, 70 mM, and 100 mM, respectively. (**B**) The secondary plot of the data from the time-course study. The equilibrium constant of GnT-III reactions was calculated by replotting [bisected]/[nonbisected] as a function of [UDP-GlcNAc]/[UDP].

UDP, and thereby enabled us to determine UDP-GlcNAc formed in the possible reverse reaction, as indicated by the elution profile of the chromatography (Figure 2D). In addition, no formation of UMP was detected during the reactions, suggesting the absence of pyrophosphatase activity which may influence the equilibrium. Aliquots of the reaction mixture were taken at appropriate time intervals, and then analyzed for the formation of both the nonbisected oligosaccharide and UDP-GlcNAc by reversed-phase and anion-exchange HPLC, respectively (Figure 2B and D). It was observed that UDP-GlcNAc was formed by the reaction of the bisected oligosaccharide substrate and UDP with GnT-III, and the increase in UDP-GlcNAc was essentially the same as the formation of the nonbisected oligosaccharide or as the loss of the bisected (Figure 3). Thus, the time-course study is consistent with the suggestion that GnT-III catalyzes bidirectional transfer of GlcNAc between the UDP and oligosaccharide.

Equilibrium state of the reversible reaction catalyzed by GnT-III

As demonstrated, a GlcNAc transfer reaction catalyzed by GnT-III is reversible and was thus found to be assessed for its equilibrium. To investigate the equilibrium state of the reversible reaction, the removal of the bisecting GlcNAc from the bisected oligosaccharide by GnT-III was monitored in the reactions with various concentrations (40, 70, 100 mM) of UDP, 0.67 μM PA-agalactosyl-bisected biantennary, and 2 μM UDP-GlcNAc. The profiles of time course showed that the formation of the nonbisected oligosaccharides reached plateau around 12 h (Figure 4A). Since the purified enzyme remained active under the conditions used, it appeared that the reactions reached equilibrium rather than lowering due to the inactivation of the enzyme. Different concentrations of UDP contained in the reactions led to distinct levels of plateau, also supporting the equilibrium of the reactions. The levels of UDP-GlcNAc produced during the reaction, 0.03 μM at the maximum, were equal to the nonbisected oligosaccharide formed (data not shown). Such an increase in the UDP-GlcNAc concentration was much less than the concentration of UDP-GlcNAc initially added to the reaction mixture, permitting approximation of the constant value for the UDP-GlcNAc concentration. Therefore, the ratio of UDP-GlcNAc to UDP, [UDP-GlcNAc]/[UDP], may be considered to be constant for each reaction. When the reaction is in equilibrium, the equilibrium constant K can be expressed as

$$K = \frac{[\text{UDP}]\,[\text{bisected}]}{[\text{UDP-GlcNAc}]\,[\text{non-bisected}]}. \quad (1)$$

Thus,

$$\frac{[\text{bisected}]}{[\text{non-bisected}]} = K\frac{[\text{UDP-GlcNAc}]}{[\text{UDP}]}. \quad (2)$$

When [bisected]/[nonbisected], whose values could be exactly determined by the chromatograms, was plotted as a function of [UDP-GlcNAc]/[UDP] (Figure 4B), the slope which was calculated by regression gives the constant. As a result, the equilibrium constant for the reactions of GnT-III, that is, the transfer of the bisecting GlcNAc between the oligosaccharide and UDP, conducted under the conditions defined was estimated to be 1.6×10^6. This value seems extraordinarily large as compared to the cases of reactions by other glycosyltransferases (Quirós et al. 2000; Chandrasekaran et al. 2008) and corresponds to 8.8 kcal/mol of the Gibbs free energy change (ΔG), which is comparable to the value for hydrolysis of ATP (Rosing and Slater 1972). The equilibrium state was also investigated by monitoring the forward reaction performed with 100 mM UDP, 0.33 μM PA-agalactosyl biantennary, and 0.125 μM UDP-GlcNAc. The profile of time course showed that the level of the bisected oligosaccharide reached plateau of 74 nM at about 6 h (data not shown). The equilibrium constant and ΔG were calculated to be 5.7×10^5 and 8.2 kcal/mol, respectively, which are consistent with the values estimated by monitoring the reverse reactions.

Preference in the removal of the bisecting GlcNAc from bisected oligosaccharides

In order to confirm that GnT-III removes the bisecting GlcNAc residues from different bisected branched oligosaccharides, PA-bisected triantennary and PA-bisected tetraantennary oligosaccharides were also used as the substrates for the reverse reaction. The purified enzyme was incubated with 3.3 μM of three PA-bisected oligosaccharides with biantennary, triantennary, and tetraantennary in the presence of 100 mM

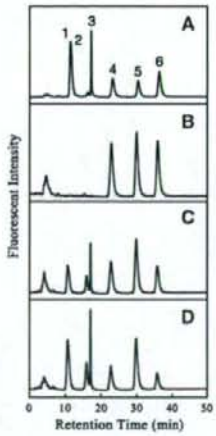

Fig. 5. Removal of the bisecting GlcNAc from various bisected oligosaccharide substrates. The purified recombinant GnT-III was incubated with 100 mM UDP and the mixture of bisected biantennary, bisected triantennary, and bisected tetraantennary oligosaccharides at 37°C. Standard oligosaccharides (**A**) and reaction products at 0 (**B**), 3 (**C**), and 6 h (**D**) were separately eluted and quantified by reversed-phase HPLC analysis. Numbers at the top represent the elution points for the oligosaccharides: 1, tetraantennary; 2, biantennary; 3, triantennary; 4, bisected biantennary; 5, bisected tetraantennary; 6, bisected triantennary.

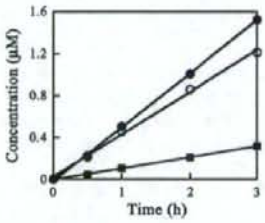

Fig. 6. Rate study for the conversion of various bisected oligosaccharide substrates. Concentrations of the reverse-reaction products were plotted against the reaction time. Opened circle, closed circle, and closed square denote biantennary, triantennary, and tetraantennary oligosaccharides, respectively.

UDP at 37°C, and the reaction products were analyzed by reversed-phase HPLC (Figure 5). The elution profiles of the products showed that GnT-III removes the bisecting GlcNAc residues from bisected triantennary and bisected tetraantennary as well as bisected biantennary, as expected by the forward reaction, the abilities of the enzyme to modify tri- and tetraantennary into bisected ones (Brockhausen et al. 1988). As shown in the profile, however, the rate of removal of the bisecting GlcNAc was different among oligosaccharide substrates, and thus it was found that GnT-III has different preference toward the bisected oligosaccharide substrates (Figure 6). Because relative rates in the reaction involving competing substrates are identical to the relative values of k_{cat}/K_m, which is a parameter to represent substrate specificity, the specificity is relatively higher for these two types of the substrate, as compared to the tetraantennary. GnT-III appears to prefer biantennary and triantennary to a similar extent, and this tendency is essentially the same as that in the forward reactions (Brockhausen et al. 1988).

Discussion

The biosynthetic pathways of *N*-linked oligosaccharides have been extensively studied, and many glycosyltransferases involved in the assembly of the sugar chains have been identified and characterized (Allen et al. 1984; Kumar et al. 1990; Tan et al. 1995; Almeida et al. 1997; Kono et al. 1997; Yanagidani et al. 1997 Sato et al. 1998). In addition to investigation of their enzymatic properties, the genes encoding these enzymes were molecularly cloned, and, as a result, the consequence of changes in their expression to the alterations of oligosaccharide structures was understood in more detail (Hennet and Ellies 1999). However, emphasized was elongation of the oligosaccharide by utilization of glycosyl donors such as nucleotide sugars, but other possible pathways of the assembly, e.g., modification by transglycosylation, had not sufficiently been examined. Recently, however, the reversible reaction of ST3Gal-II was investigated (Chandrasekaran et al. 2008), and it was suggested that terminal sialic acid residues can be intermolecularly propagated by transglycosylation involving CMP but not CMP-Sia. Thus, for a better understanding of the biosynthesis of glycoconjugates, it would be required to consider bidirectional reactions of glycosyltransferases, which are attachment and removal of carbohydrate moieties.

The present study was conducted in order to examine whether GnT-III is actually capable of catalyzing the reverse reaction in which a GlcNAc residue is transferred from an oligosaccharide to nucleotide to yield the corresponding nucleotide sugar. The results obtained clearly showed that the reactions catalyzed by GnT-III are reversible. However, while the reverse reaction catalyzed by ST3Gal-II appeared to proceed comparably to the forward reaction (Chandrasekaran et al. 2008), it seems more likely that the reaction by GnT-III is essentially irreversible in vivo, as judged by the suggestion that the equilibrium of the reaction greatly prefers the formation of the bisecting GlcNAc. The intracellular or intra-Golgi concentration of UDP, expected as much as a few mM level (Murphy et al. 1973; Fleischer 1981; Waldman and Rudnick 1990), must be too low to reversely drive the reaction by GnT-III toward the removal of the bisecting GlcNAc. These findings suggest that the reaction by GnT-III is very ridged against perturbation in terms of equilibrium and is likely to be resistant to fluctuating changes of a factor such as the UDP level which is a driving force toward the removal of the bisecting GlcNAc. It is well known that the addition of the bisecting GlcNAc induces the conformational change (Brisson and Carver 1983a, 1983b; Taniguchi et al. 1996) and probably energetic stabilization of the oligosaccharide structure. The energetic stability of the bisected oligosaccharide appears to contribute to displacement of the equilibrium toward the formation of the bisecting GlcNAc.

In many other glycosyltransferases involved in the *N*-linked oligosaccharide biosynthesis, the reversible reactions and their equilibrium states have not yet examined. Because various glycosyltransferases use UDP-sugars as the donor for their reactions, similarly to GnT-III, alteration in the level of UDP in the Golgi apparatus may have effects on the glycosyltransferase reactions by perturbing the equilibrium. The extent of such an effect depends on the equilibrium constant for each glycosyltransferase-catalyzed reaction. In the case of a glycosyltransferase with the equilibrium constant much less than the value for GnT-III, the synthesis of the structure by the former

enzyme would be readily decreased by the transition to a new equilibrium as a result of the increase in the UDP level, relative to that of the bisecting GlcNAc by GnT-III, since the reaction by GnT-III is expected to almost constantly proceed regardless of the change in the UDP level. As a result, a dominant synthetic pathway in cells might be changed to different one. This type of the control could play a significant role in the fine-tuning of the biosynthesis of sugar chains and/or a possible regulation mechanism which is independent of gene expression of glycosyltransferases.

It would be generally accepted that one specific structure would be synthesized more by increased expression of the responsible glycosyltransferase whereas the increase in the level of other structure depends on an expression of different enzyme (Kagawa et al. 1988). Therefore, a ultimate structure of the oligosaccharide can be determined according to the overall expression pattern of all glycosyltransferases involved in its assembly because parallel, sequential and/or competing reactions, all of which constitute the biosynthetic pathways of the oligosaccharide, should be controlled by relative magnitude in reaction rates. In fact, such an idea has reasonably explained assembly and syntheses of many oligosaccharides (Ikeda et al. 2000; Sasai et al. 2002; Montiel et al. 2003; Ramasamy et al. 2005). However, if a reversible reaction by glycosyltransferase is actually involved in the formation of a variety of oligosaccharide structures, as suggested for the case of terminal sialylation, it may be required to consider "equilibrium control," in conjunction with "rate control," in the biosyntheses of oligosaccharides.

Material and methods

Expression and purification of the recombinant GnT-III

The recombinant baculovirus encoding rat GnT-III was prepared as described previously (Ikeda et al. 2000). Approximately, 1.5×10^7 Sf21 cells were seeded per 150 cm^2 culture flask (Greiner Bio One GmbH, Frickenhausen, Germany) with 20 mL of Sf-900™ II SFM (Gibco, Carlsbad, CA), and then infected with the recombinant baculovirus at sufficiently high multiplicity of infection. After incubation at 27°C for 96 h, the culture medium, which contained the secreted recombinant GnT-III, was dialyzed against a 20 mM sodium phosphate buffer (pH 6.5) and applied onto ion-exchange chromatography using CM Sepharose (GE Healthcare Bio-Sciences, Piscataway, NJ). The recombinant enzyme was eluted with the 20 mM sodium phosphate buffer (pH 6.5) containing 0.5 M sodium chloride, followed by further purification by nickel-chelating affinity chromatography. The protein, which was applied to a Ni^{2+}-charged Chelating Sepharose column (GE Healthcare Bio-Sciences), was eluted with the 50 mM sodium phosphate buffer (pH 6.5) containing 0.5 M sodium chloride, 0.2% Triton X-100, and 0.2 M EDTA. The eluted fraction was dialyzed against the 20 mM sodium phosphate buffer (pH 6.5) containing 0.1% Triton X-100 and finally concentrated with Centricon Ultracel YM-10 (Millipore, Billerica, MA).

Protein determination

The protein concentration was determined by a bicinchoninic acid method using BCA Protein Assay Reagent (Pierce Biotechnology, Rockford, IL) according to the procedures recommended by the supplier. Bovine serum albumin was used as the standard protein.

Preparation of pyridylaminated-bisected oligosaccharides

PA-bisected oligosaccharides were prepared by the enzymatic conversion of PA-agalactosyl biantennary, 2,4-branched triantennary, and tetraantennary oligosaccharides (TaKaRa Bio, Shiga, Japan) using the recombinant GnT-III. The reactions were carried out in a 15 μL of solution containing 125 mM MES-NaOH (pH 6.25), 10 mM $MnCl_2$, 0.5% Triton X-100, 20 mM UDP-GlcNAc, 10 μM PA-oligosaccharide, and 1 μL of concentrated GnT-III (approximately 0.18 μg/μL), at 37°C for 6 h. The reaction mixture was boiled, and centrifuged at 15,000 rpm for 10 min. The resulting supernatant was applied to reversed-phase HPLC using the Alliance HPLC system (Waters, Eschborn, Germany) equipped with a TSK-gel ODS 80-TM column (4.6 × 150 mm, Tosoh, Tokyo, Japan). PA-bisected oligosaccharides were eluted at a flow rate of 1 mL/min using a gradient consisting of solvent A (20 mM acetate buffer, pH 4.0) and solvent B (20 mM acetate buffer containing 1% butanol, pH 4.0). The gradient was made by increasing the proportion of solvent B (10% (0–5 min), 25% (45 min), 10% (46–50 min)). The elution was monitored by fluorescence at Ex = 310 nm and Em = 380 nm. The fluorescent fractions were collected and dried prior to activity assays.

Assay of GnT-III activity

For a forward reaction in which GlcNAc is transferred to an oligosaccharide substrate from UDP-GlcNAc, the assay was carried out, essentially as described previously (Nishikawa et al. 1988; 1990; Taniguchi et al. 1989). Briefly, the PA-biantennary oligosaccharide was incubated at 37°C with the recombinant GnT-III and 20 mM UDP-GlcNAc in the 125 mM MES-NaOH buffer (pH 6.25) containing 10 mM $MnCl_2$ and 0.5% Triton X-100. After appropriate time of incubation, the reaction mixture was boiled, and then centrifuged at 15,000 rpm for 10 min. The resulting supernatant was analyzed by reversed-phase HPLC using the Alliance HPLC system equipped with a TSK-gel ODS 80-TM column (4.6 × 150 mm). PA-bisected biantennary and PA-biantennary oligosaccharides were separately eluted in an isocratic manner with the 20 mM ammonium acetate buffer containing 0.3% butanol (pH 4.0) at a flow rate of 1 mL/min and monitored by a fluorescence detector using Ex = 310 nm and Em = 380 nm. A reverse reaction which removes the bisecting GlcNAc residue from the oligosaccharide was also analyzed as carried out for the forward, described above, except respective replacements of the nonbisected oligosaccharide and UDP-GlcNAc by the bisected PA-oligosaccharide and UDP.

Measurement of UDP-GlcNAc

UDP-GlcNAc formed in the reaction mixture was analyzed by anion-exchange HPLC using the Alliance HPLC system equipped with a Partisil-10 SAX column (4.6 × 250 mm, Millipore, Billerica, MA) as described previously (ap Rees et al. 1984; Beckles et al. 2001; Jenner et al. 2001). UDP-GlcNAc was eluted separately from UDP at a flow rate of 1 mL/min using a gradient consisting of buffer A (40 mM potassium phosphate buffer, pH 3.0) and buffer B (0.2 M potassium phosphate buffer containing 0.75 M potassium chloride, pH 2.8) by increasing the proportion of buffer B (0% (0–2 min), 35% (20–30 min), 0%

(31–40 min)). Eluted UDP and UDP-GlcNAc were monitored by absorbance at 254 nm. The formation of UDP-GlcNAc was determined from a calibration curve by standard samples.

Data analysis and curve fitting

When the time course of the conversion of PA-oligosaccharides was assessed to characterize the equilibrium state of the reactions catalyzed by GnT-III, the data obtained were fitted to a single exponential curve. The enzyme reactions examined may be approximated to a modified pseudo first-order kinetic model, as described by Eq. (3), under the conditions used:

$$[P]_t = [S]_0 \left\{1 - \frac{k'}{k+k'} - \frac{k}{k+k'} \exp[-(k+k')t]\right\}. \quad (3)$$

In the bidirectional reaction to be examined, $[P]_t$ and $[S]_0$ denote the concentration of the product at time t and the initial concentration of the substrate, respectively. Apparent first-order kinetic constants for the forward and reverse reactions are denoted by k and k', respectively. Data fitting and drawing the theoretical curves were performed by a nonlinear regression analysis with Prism 4 software for Macintosh (Graph Pad Software, Inc., San Diego, CA). The equilibrium point for each of the defined conditions was also calculated, and the equilibrium constant was estimated by a linear regression in the secondary plot.

Removal of the bisecting GlcNAc from the bisected oligosaccharide mixture

The removal of bisecting GlcNAc residue from the PA-bisected oligosaccharide mixture was carried out in a 15 μL solution containing 125 mM MES-NaOH (pH 6.25), 10 mM $MnCl_2$, 0.5% Triton X-100, 100 mM UDP, 3.3 μM PA-bisected biantennary, 3.3 μM PA-bisected triantennary, 3.3 μM PA-bisected tetraantennary, and 0.5 μL of concentrated GnT-III (approximately 0.56 μg/μL), at 37°C for 6 h. After appropriate time of incubation, 1.5 μL of the reaction mixture was collected, boiled, and centrifuged at 15,000 rpm for 10 min. The resulting supernatant was analyzed by reversed-phase HPLC using the Alliance HPLC system equipped with a TSK-gel ODS 80-TM column (4.6 × 150 mm), and bisected and nonbisected oligosaccharides were separately eluted as described in *Preparation of PA-bisected oligosaccharides*.

Electrospray ionization mass spectrometry

Electrospray ionization mass spectrometry (ESI-MS) was carried out using an LCQ (Finnigan) quadrupole mass spectrometer equipped with an electrospray atmospheric pressure ionization source (Thermo Scientific, Waltham, MA). The PA-oligosaccharide was dissolved in a 50% aqueous methanol solution containing 1% acetic acid and introduced into the ion source by a direct infusion at a flow rate of 3 μL/min using a syringe pump integrated into the system. ESI-MS spectra were obtained using the positive ion mode. The ion spray voltage and capillary voltage were 4.5 kV and 10 V, respectively, and capillary temperature was 200°C. Full scan spectra were obtained in the range of 600–2000.

Funding

Core Research for Evolutional Science and Technology (CREST) of the Japan Science and Technology Agency.

Conflict of interest statement

None declared.

Abbreviations

ATP, adenosine-triphosphate; CMP, cytidine-monophosphate, CMP-Sia, cytidine-monophosphate-sialic acid; ESI-MS, electrospray ionization mass spectrometry; GlcNAc, *N*-acetylglucosamine; HPLC, high-performance liquid chromatography; MES, 2-(*N*-morpholino) ethane sulfonic acid; NDP, nucleoside-diphosphate; UDP, uridine diphosphate; UDP-GlcNAc, uridine-diphospho-*N*-acetylglucosamine; UMP, uridine monophosphate.

References

Allen SD, Tsai D, Schachter H. 1984. Control of glycoprotein synthesis. The in vitro synthesis by hen oviduct membrane preparations of hybrid asparagine-linked oligosaccharides containing 5 mannose residues. *J Biol Chem*. 259(11):6984–6990.

Almeida R, Amado M, David L, Levery SB, Holmes EH, Merkx G, van Kessel AG, Rygaard E, Hassan H, Bennett E, et al. 1997. A family of human β4-galactosyltransferases. Cloning and expression of two novel UDP-galactose:β-*N*-acetylglucosamine β1,4-galactosyltransferases, β4Gal-T2 and β4Gal-T3. *J Biol Chem*. 272(51):31979–31991.

ap Rees T, Leja M, Macdonald FD, Green JH. 1984. Nucleotide sugars and starch synthesis in the spadix of *Arum maculatum* and suspension cultures of *Glycine max*. *Phytochemistry*. 23(11):2463–2468.

Beckles DM, Smith AM, ap Rees T. 2001. A cytosolic ADP-glucose pyrophosphorylase is a feature of graminaceous endosperms, but not of other starch-storing organs. *Plant Physiol*. 125(2):818–827.

Bendiak B, Schachter H. 1987. Control of glycoprotein synthesis. Kinetic mechanism, substrate specificity, and inhibition characteristics of UDP-*N*-acetylglucosamine:α-D-maannoside β1-2 *N*-acetylglucosaminyltransferase II from rat liver. *J Biol Chem*. 262(12):5784–5790.

Breton C, Snajdrova I, Jeanneau C, Koca J, Imberty A. 2006. Structures and mechanisms of glycosyltransferases. *Glycobiology*. 16(2):29R–37R.

Brisson JR, Carver JP. 1983a. Solution conformation of asparagines-linked oligosaccharides: α(1-2)-, α(1-3)-, β(1-2)- and β(1-4)-linked units. *Biochemistry*. 22(15):3671–3680.

Brisson JR, Carver JP. 1983b. Solution conformation of asparagines-linked oligosaccharides: α(1-6)-linked moiety. *Biochemistry*. 22(15):3680–3686.

Brockhausen I, Carver JP, Schachter H. 1988. Control of glycoprotein synthesis. The use of oligosaccharide substrates and HPLC to study the sequential pathway for *N*-acetylglucosaminyltransferases I, II, III, IV, V, and VI in the biosynthesis of highly branched *N*-glycans by hen oviduct membranes. *Biochem Cell Biol*. 66(10):1134–1151.

Bulter T, Wandrey C, Elling L. 1997. Chemoenzymatic synthesis of UDP-*N*-acetyl-α-D-galactosamine. *Carbohydr Res*. 305(3):469–473.

Chandrasekaran EV, Xue J, Xia J, Locke RD, Matta KL, Neelamegham S. 2008. Reversible sialylation: Synthesis of cytidine 5′-monophospho-*N*-acetylneuraminic acid from cytidine 5′-monophosphate with α2,3-sialyl *O*-glycan-, glycolipid-, and macromolecule-based donors yields diverse sialylated products. *Biochemistry*. 47(1):320–330.

Cuypers HT, ter Haar EM, Jansen PL. 1984. UDP-glucuronyltransferase-catalyzed deconjugation of bilirubin monoglucuronide. *Hepatology*. 4(5):918–922.

Deangelis PL, Oatman LC, Gay DF. 2003. Rapid chemoenzymatic synthesis of monodisperse hyaluronan oligosaccharides with immobilized enzyme reactors. *J Biol Chem*. 278(37):35199–35203.

Fleischer B. 1981. The nucleotide content of rat liver Golgi vesicles. *Arch Biochem Biophys*. 212(2):602–610.

Gleeson PA, Schachter H. 1983. Control of glycoprotein synthesis. *J Biol Chem.* 258(10):6162–6173.

Hennet T, Ellies LG. 1999. The remodeling of glycoconjugates in mice. *Biochim Biophys Acta.* 1473(1):123–136.

Ikeda Y, Koyota S, Ihara H, Yamaguchi Y, Korekane H, Tsuda T, Sasai K, Taniguchi N. 2000. Kinetic basis for the donor nucleotide-sugar specificity of β1,4-*N*-acetylglucosaminyltransferase III. *J Biochem.* 128(4):609–619.

Jenner HL, Winning BM, Millar AH, Tomlinson KL, Leaver CJ, Hill SA. 2001. NAD malic enzyme and the control of carbohydrate metabolism in potato tubers. *Plant Physiol.* 126(3):1139–1149.

Kagawa Y, Takasaki S, Utsumi J, Hosoi K, Shimizu H, Kochibe N, Kobata A. 1988. Comparative study of the asparagines-linked sugar chains of natural human interferon-β1 and recombinant human interferon-β1 produced by three different mammalian cells. *J Biol Chem.* 263(33):17508–17515.

Koeller KM, Wong CH. 2000. Synthesis of complex carbohydrates and glycoconjugates: Enzyme-based and programmable one-pot strategies. *Chem Rev.* 100(12):4465–4494.

Kono M, Ohyama Y, Lee YC, Hamamoto T, Kojima N, Tsuji S. 1997. Mouse β-galactoside α2,3-sialyltransferases: Comparison of in vitro substrate specificities and tissue specific expression. *Glycobiology.* 7(4):469–479.

Koyota S, Ikeda Y, Miyagawa S, Ihara H, Koma M, Honke K, Shirakura R, Taniguchi N. 2001. Down-regulation of the α-Gal epitope expression in *N*-glycans of swine endothelial cells by transfection with the *N*-acetylglucosaminyltransferase III gene. *J Biol Chem.* 276(35):32867–32874.

Kumar R, Yang J, Larsen RD, Stanley P. 1990. Cloning and expression of *N*-acetylglucosaminyltransferase I, the medial Golgi transferase that initiates complex *N*-linked carbohydrate formation. *Proc Natl Acad Sci USA.* 87(24):9948–9952.

Lairson LL, Henrissat B, Davies GJ, Withers SG. 2008. Glycosyltransferases: Structures, functions, and mechanisms. *Annu Rev Biochem.* 77:521–555.

Miller KD, Guyon V, Evans JN, Shuttleworth WA, Taylor LP. 1999. Purification, cloning, and heterologous expression of a catalytically efficient flavonol 3-*O*-galactosyltransferase expressed in the male gametophyte pf *Petunia hybrida*. *J Biol Chem.* 274(48):34011–34019.

Minami A, Kakinuma K, Eguchi T. 2005. Aglycon switch approach toward unnatural glycosides from natural glycoside with glycosyltransferase VinC. *Tetrahedron Lett.* 46(37):6187–6190.

Montiel MD. Krzewinski-Recchi MA, Delannoy P, Harduin-Lepers A. 2003. Molecular cloning, gene organization and expressions of the human UDP-GalNAc:Neu5Acα2-3Galβ-R β1,4-*N*-acetylgalactosyltransferase responsible for the biosynthesis of the blood group Sda/Cad antigen: Evidence for an unusual extended cytoplasmic domain. *Biochem J.* 373(Pt 2):369–379.

Murphy G, Ariyanayagam AD, Kuhn NJ. 1973. Progesterone and the metabolic control of the lactose biosynthetic pathway during lactogenesis in the rat. *Biochem J.* 136(4):1105–1116.

Narashimhan S. 1982. Control of glycoprotein synthesis. UDP-GlcNAc: glycopeptide β4-*N*-acetylglucosaminyltransferase III, an enzyme in hen oviduct which adds GlcNAc in β1-4 linkage to the β-linked mannose of the trimannosyl core of *N*-glycosyl oligosaccharides. *J Biol Chem.* 257(17):10235–10242.

Nishikawa A, Fujii S, Sugiyama T, Taniguchi N. 1988. A method for the determination of *N*-acetylglucosaminyltransferase III activity in rat tissues involving HPLC. *Anal Biochem.* 170(2):349–354.

Nishikawa A, Gu J, Fujii S, Taniguchi N. 1990. Determination of *N*-acetylglucosaminyltransferases III, IV and V in normal and hepatoma tissues of rats. *Biochem Biophys Acta.* 1035(3):313–318.

Nishikawa A, Ihara Y, Hatakeyama M, Kangawa K, Taniguchi N. 1992. Purification, cDNA cloning, and expression of UDP-*N*-acetylglucosamine: β-D-mannoside β-1,4-*N*-acetylglucosaminyltransferase III from rat kidney. *J Biol Chem.* 267(25):18199–18204.

Peters WH, Jansen PL, Cuypers HT, de Abreu RA, Nauta H. 1986. Deconjugation of glucuronides catalysed by UDPglucuronyltransferase. *Biochim Biophys Acta.* 873(2):252–259.

Quirós LM, Carbajo RJ, Braña AF, Salas JA. 2000. Glycosylation of macrolide antibiotics. Purification and kinetic studies of a macrolide glycosyltransferase from *Streptomyces antibioticus*. *J Biol Chem.* 275(16):11713–11720.

Ramasamy V, Ramakrishnan B, Boeggeman E, Ratner DM, Seeberger PH, Qasba PK. 2005. Oligosaccharide preferences of β1,4-galactosyltransferase-I: Crystal structures of Met340His mutant of human β1,4-galactosyltransferase-I with a pentasaccharide and trisaccharides of the *N*-glycan moiety. *J Mol Biol.* 353(1):53–67.

Rosing J, Slater EC. 1972. The value of G degrees for the hydrolysis of ATP. *Biochim Biophys Acta.* 267(2):275–290.

Sasai K, Ikeda Y, Fujii T, Tsuda T, Taniguchi N. 2002. UDP-GlcNAc concentration is an important factor in the biosynthesis of β1,6-branched oligosaccharides: Regulation based on the kinetic properties of *N*-acetylglucosaminyltransferase V. *Glycobiology.* 12(2):119–127.

Sato T, Furukawa K, Bakker H, Van den Eijnden DH, Van Die I. 1998. Molecular cloning of a human cDNA encoding β-1,4-galactosyltransferase with 37% identity to mammalian UDP-Gal:GlcNAc β-1,4-galactosyltransferase. *Proc Natl Acad Sci USA.* 95(2):472–477.

Schachter H. 1986. Biosynthesis controls that determine the branching and microheterogeneity of protein-bound oligosaccharides. *Biochem Cell Biol.* 64(3):163–181.

Schachter H, Narasimhan S, Gleeson P, Vella G. 1983. Control of branching during the biosynthesis of asparagines-linked oligosaccharides. *J Biochem Cell Biol.* 61(9):1049–1066.

Sears P, Wong CH. 2001. Toward automated synthesis of oligosaccharides and glycoproteins. *Science.* 291(5512):2334–2350.

Tan J, D'Agostaro AF, Bendiak B, Reck F, Sarkar M, Squire JA, Leong P, Schachter H. 1995. The human UDP-*N*-acetylglucosamine: α-6-D-Mannoside-β-1,2-*N*-acetylglucosaminyltransferase II gene (MGAT2). Cloning of genomic DNA, localization to chromosome 14q21, expression in insect cells and purification of the recombinant protein. *Eur J Biochem.* 231(2):317–328.

Taniguchi N, Nishikawa A, Fujii S, Gu JG. 1989. Glycosyltransferase assays using pyridylaminated acceptors: *N*-Acetylglucosaminyltransferase III, IV, and V. *Methods Enzymol.* 179:397–408.

Taniguchi N, Yoshimura M, Miyoshi E, Ihara Y, Nishikawa A, Fujii S. 1996. Remodeling of cell surface glycoproteins by *N*-acetylglucosaminyltransferase III gene transfection: Modulation of metastatic potentials and down regulation of hepatitis B virus replication. *Glycobiology.* 6(7):691–694.

Wacker M, Linton D, Hitchen PG, Nita-Lazar M, Haslam SM, North SJ, Panico M, Morris HR, Dell A, Wren BW, et al. 2002. *N*-Linked glycosylation in *Campylobacter jejuni* and its functional transfer into *E. coli*. *Science.* 298(5599):1790–1793.

Waldman BC, Rudnick G. 1990. UDP-GlcNAc transport across the Golgi membrane: Electroneural exchange for dianionic UMP. 29(1):44–52.

Yanagidani S, Uozumi N, Ihara Y, Miyoshi E, Yamaguchi N, Taniguchi N. 1997. Purification and cDNA cloning of GDP-L-Fuc:*N*-acetyl-β-D-glucosaminide:α1-6 fucosyltransferase (α1-6 FucT) from human gastric cancer MKN45 cells. *J Biochem.* 121(3):626–632.

Zhang C, Griffith BR, Fu Q, Albermann C, Fu X, Lee IK, Li L, Thorson JS. 2006. Exploiting the reversibility of natural product glycosyltranferase-catalyzed reactions. *Science.* 313(5791):1291–1294.

Journal of Biochemistry Advance Access published January 29, 2009

Requirement of Fut8 for the expression of vascular endothelial growth factor receptor-2: a new mechanism for the emphysema-like changes observed in Fut8-deficient mice

Xiangchun Wang[1], Tomohiko Fukuda[2], Wenzhe Li[3,4], Cong-xiao Gao[1], Akihiro Kondo[3], Akio Matsumoto[1], Eiji Miyoshi[5], Naoyuki Taniguchi[1,6,*] and Jianguo Gu[2,*]

From the [1]Department of Disease Glycomics, Institute for Microbial Diseases, Osaka University, 2-1 Yamadaoka, Suita, Osaka 565-0871 Japan; [2]Division of Regulatory Glycobiology, Tohoku Pharmaceutical University, 4-4-1 Komatsusima, Aobaku, Sendai, Miyagi 981-8558 Japan; [3]Department of Glycotherapeutics, Osaka University Graduate School of Medicine, B1, 2-2 Yamadaoka, Suita, Osaka 565-0871, Japan; [4]Key Laboratory of Bio-organic Chemistry, College of Bioengineering, Dalian University, Dalian 116622, China; [5]Department of Molecular Biochemistry and Clinical Investigation, Division of Health Science, Osaka University Graduate School of Medicine, 1-7 Yamadaoka, Suita, Osaka 565-0871 Japan; [6]Systems Glycobiology Group, Disease Glycomics Team, RIKEN, Wako 351-0198, Japan

[*] To whom all correspondence should be addressed. Department of Disease Glycomics, Institute for Microbial Diseases, Osaka University, 4th Floor, Center for Advanced Science and Innovation, Osaka University, 2-1 Yamadaoka Suita, Osaka 565-0871, Japan; E-mail: tani52@wd5.so-net.ne.jp; or Division of Regulatory Glycobiology, Tohoku Pharmaceutical University, 4-4-1 Komatsushima, Aobaku, Sendai, Miyagi 981-8558, Japan Tel: 81-22-727-0216; Fax: 81-22-727-0078; E-mail: jgu@tohoku-pharm.ac.jp

Running title: Fut8 is required for VEGFR-2 expression

Abstract

α1,6-Fucosylation plays key roles in many biological functions, as evidenced by the study of α1,6-fucosyltransferase (*Fut8*)-knockout (*Fut8*$^{-/-}$) mice. Phenotypically, *Fut8*$^{-/-}$ mice exhibit emphysema-like changes in the lung, and severe growth retardation. *Fut8*$^{-/-}$ cells also show marked dysregulation of the TGF-β1 receptor, EGF receptor, integrin activation and intracellular signaling, all of which can be rescued by reintroduction of *Fut8*. The results of the present study demonstrated that vascular endothelial growth factor receptor-2 (VEGFR-2) expression was significantly suppressed in *Fut8*$^{-/-}$ mice, suggesting that *Fut8* was required for VEGFR-2 expression. The expression of VEGFR-2 mRNA and protein was consistently down regulated by knockdown of the *Fut8* gene with small interference RNA in A549 cells, as well as in TPG49 cells, suggesting that suppression occurs at the level of transcription. In contrast, the expression level of ceramide, an inducer of cell apoptosis, was increased in the lungs of *Fut8*$^{-/-}$ mice. The terminal transferase dUTP nick end-labeling (TUNEL) assay was used to identify apoptotic cells. The number of TUNEL-positive septal epithelia and endothelia cells was significantly increased in the alveolar septa of lungs from *Fut8*$^{-/-}$ mice when in comparison with lungs from wild type mice. It is well known that, in emphysema, ceramide expression can be greatly enhanced by blockade of the VEGFR-2. Thus, suppression of VEGFR-2 expression may provide a novel explanation for the emphysema-like changes in *Fut8*$^{-/-}$ mice.

Key words: apoptosis, emphysema, fucosylation, Fut8, VEGFR-2 expression

Introduction

α1,6-fucosyltransferase (*Fut8*) catalyzes the transfer of a fucose residue from GDP-fucose to position 6 of the innermost GlcNAc residue to form α1,6-fucose in hybrid and complex types of *N*-linked oligosaccharides of glycoproteins (1) (Fig. 6A). α1,6-fucosylated glycoproteins are widely distributed in mammalian tissues, and the process of the α1,6-fucosylation is altered under pathological conditions, such as hepatocellular carcinoma and liver cirrhosis (2,3). It also has been reported that the deletion of α1,6-fucose from the IgG1 molecule enhances antibody-dependent cellular cytotoxicity (ADCC) activity 50- to 100-fold. This observation indicates that the α1,6-fucose is an important sugar chain for ADCC activity (4,5). Recently, the physiological functions of α1,6-fucose have been further investigated by our group using Fut8-deficient mice (6). *Fut8* knockout (*Fut8*$^{-/-}$) mice showed severe growth retardation and the mortality rate was ~70 % during the first 3 postnatal days. Surviving mice suffered from emphysema-like changes in the lungs that appeared to be due, in part, to a lack of α1,6-fucosylation of the TGF-β1 receptor, which consequently results in marked dysregulation of TGF-β1 receptor activation and signaling. Moreover, the loss of α1,6-fucosylation results in down-regulation of EGF receptor-mediated cellular signaling pathways, as well as of integrin α3β1-mediated cell adhesion (7,8). Taken together, these results suggest that α1,6-fucose plays a key role in regulating important physiological functions via modification of functional proteins (9,10).

Emphysema is a major contributor to the morbidity and mortality associated with chronic obstructive pulmonary disease (COPD), a highly prevalent lung disease, for which there is no effective treatment. Chronic cigarette smoking is the most important risk factor for this global health problem. The hypothesis that cigarette smoking causes emphysema by stimulating inflammatory cells and by inducing production of proteinases, is most relevant. In fact, this